Mississippi waters reaching South Florida reefs under no flood conditions: Synthesis of observing and modeling system findings

Matthieu Le Hénaff[1,2*]
Vassiliki H. Kourafalou[3]

[1]University of Miami/Cooperative Institute for Marine and Atmospheric Studies (CIMAS)
4600 Rickenbacker Causeway, Miami, FL 33149-1098, USA

[2]NOAA/Atlantic Oceanographic and Meteorological Laboratory (AOML)
4301 Rickenbacker Causeway, Miami, FL 33149, USA

[3]University of Miami/Rosenstiel School of Marine and Atmospheric Science (RSMAS)
4600 Rickenbacker Causeway, Miami, FL 33149-1098, USA

*Contact author: Matthieu Le Hénaff
Tel: (1) 305 421 4154
Fax: (1) 305 421 4221
Email: matthieu.lehenaff@noaa.gov

for publication in

Ocean Dynamics

Abstract

In August 2014, *in situ* measurements revealed an intense salinity drop impacting South Florida coral reefs, between Pulley Ridge (Southwest Florida Shelf) and the Florida Keys. The low salinity waters had a surface signal of 32 (down from 35.2) and extended over a 15-20 m deep lens. Satellite observations showed that this abrupt drop in salinity was due to a southeastward export of Mississippi River waters from the Northern Gulf of Mexico (GoM), revealing strong interaction between coastal and oceanic flows. Unlike previous events of marked long-distance Mississippi water export, this episode is not associated with Mississippi flooding conditions, which makes it a unique study case.

We have developed a high-resolution (~2 km) comprehensive hydrodynamic numerical model of the GoM to study the conditions that controlled the 2014 Mississippi River water export episode. It is based on the HYbrid Coordinate Ocean Model (HYCOM) and assimilates remotely sensed altimetry and sea surface temperature observations, to ensure that the simulated upper-ocean is realistic. This regional model has a detailed representation of coastal physics (especially river plume dynamics) and employs high frequency river discharge and atmospheric forcing. The combined use of the simulation and observations reveals a unique pathway that brought Mississippi waters first eastward along the Northern GoM continental shelf, under prevailing winds and the presence of an anticyclonic Loop Current Eddy, then southward along the edge of the West Florida Shelf, before reaching the deep GoM. Unlike usually observed, the offshore advection of Mississippi River waters thus took place far from the Delta area, which is another specificity of the 2014 episode. Finally, in the Florida Straits, Mississippi waters were advected from the deep ocean to the continental shelf under the influence of both deep sea (particularly a cyclonic Loop Current frontal eddy) and shelf flows (wind-induced Ekman transport). The simulation, in tandem with

data, thus helped analyze processes that are likely to affect the connectivity between reefs in the southern Florida region (Florida Keys, Dry Tortugas, Pulley Ridge) and remote areas (Mississippi Delta), as well as the local connectivity between neighboring reefs.

1. Introduction

The Mississippi River (MR) is the largest river in North America, with an average discharge of ~13,500 m^3/s (Hu et al., 2005). The MR is a major source of freshwater, but also of nitrates and organic matter for the Gulf of Mexico (GoM). As such, it is a major provider of nutrients, responsible for the high productivity observed in the Northern GoM (Rabalais et al., 1991). The MR discharge is usually large in late winter and spring, following the run-off from continental ice, and can be associated with hypoxia episodes downstream the MR plume, on the Louisiana-Texas (LATEX, Figure 1) shelf, due to the decomposition of the large quantities of organic carbon from river origin (Rabalais et al., 2002). Beyond the shelf, the MR is also a major source of nutrients for the deep GoM. Indeed, the impact of MR waters can be felt at long distances from the Mississippi Delta, in particular when they are entrained along the Loop Current (LC) when it is extended far northward into the GoM. The LC is a branch of the North Atlantic western boundary current, which later forms the Gulf Stream. Episodes of such LC entrainment were documented in the past, and were associated with the presence of MR waters as far as the Florida Keys area, or even further downstream the Gulf Stream along the southeastern U.S. (Ortner et al., 1995; Gilbert et al., 1996; Hu et al., 2005; Schiller and Kourafalou, 2014). The LC can thus provide nutrients to the Florida Keys, which host the largest coral reefs in the continental U.S., and as such it is a vector of connectivity between the Mississippi Delta area and South Florida ecosystems. The overarching goal of this study is to combine observations (both *in situ* and satellite) and high-resolution, data

assimilative modeling to elucidate the conditions and processes leading to the export of Mississippi waters from the Delta to South Florida coastal areas.

The first well-studied episode of long-distance MR water export took place in 1993, following major MR floods in spring and summer (Ortner et al., 1995; Gilbert et al., 1996). During the 1993 event, *in situ* measurements showed that MR waters were advected along the LC, in a quasi-direct route, from the Mississippi Delta area to the Florida Straits, where they were observed in early September, then further down along the Gulf Stream on the Atlantic coast of the US in mid-to-late September. Sea surface salinity, usually around 36, dropped to less than 32 in the Florida Straits at the time; the low-salinity layer at the surface, associated with this MR water export, was estimated to be about 20 m thick in the Florida Straits (Ortner et al., 1995; Gilbert et al., 1996). A NOAA report by Dowgiallo (1994) presents some additional data, indicating the presence of low-salinity surface waters on the West Florida Shelf (WFS) in August and in October, 1993, presumably under the influence of the extended LC. In summer 2011, filaments of high chlorophyll-a (chl-a) have been observed to be advected from the Mississippi Delta to the Florida Straits (Androulidakis and Kourafalou, 2013), although no report based on *in situ* salinity measurements is available to indicate the magnitude of its effect in the Florida Straits. Both episodes are associated with reported flooding conditions, which have long been considered necessary for the export of vast amounts of MR waters toward the GoM interior and South Florida, along with an extended LC (Ortner et al., 1995). Another MR export episode was reported in 2004, but with much smaller salinity drop (from 36.2 to 35.6) along the Florida Keys (Hu et al., 2005; Schiller and Kourafalou, 2014). A novel aspect of our study is to document observational evidence and further study similar processes, in the absence of MR flooding conditions.

Recent studies have focused on the dynamics of the MR plume in the Northern GoM. The natural pathway for the buoyant MR plume is to turn anticyclonically to the west and follow the coastline toward the LATEX shelf (Walker, 1996; Kourafalou and Androulidakis, 2013). This westward pathway is due to the balance between the cross-shore pressure gradient (due to the fresher coastal waters) and the Coriolis force; it forms the "downstream" major buoyancy-driven current, in the direction of Kelvin wave propagation (Kourafalou et al., 1996). In addition, the MR plume can experience different pathways under additional forcing mechanisms, in particular winds on the shelf and offshore flows. Southerly and southwesterly winds (upwelling favorable), which are common in spring and summer over the Northern GoM, are associated with an eastward advection of the MR plume (Morey et al., 2003a,b; Schiller et al., 2011). This pathway toward the opposite direction of the downstream flow has been identified as the "upstream" plume pathway, here toward the Mississippi-Alabama-Florida (MAFLA, Figure 1) shelf (Kourafalou et al., 1996; Kourafalou and Androulidakis, 2013). Strong upwelling conditions lead to strengthening the upstream current and often eliminate the downstream flow. On the other hand, downwelling favorable winds (strong easterly component) have the opposite effect, resulting in the strongest downstream transport conditions (Kourafalou and Androulidakis, 2013). On the WFS, model studies have identified a southward current that could favor the transport of low salinity waters present in the Northeastern GoM in spring. He and Weisberg (2002) found that such a current could be established in spring over the western part of the WFS. This potential shelf route for the southward advection of MR waters in the GoM is also mentioned in Weisberg et al. (2005), but it has never been actually observed in the case of long-distance MR water export episode. Another novel aspect of our study is to employ a unique set of observations that confirms model-based findings.

Another important mechanism forcing the MR plume is the interactions with deep GoM flows; this is corroborated by the very narrow continental shelf in the vicinity of the Mississippi Delta (Walker et al., 2005; Morey et al., 2003b; Schiller et al., 2011). The deep GoM dynamics are dominated by the LC and the associated eddy field. The LC has a highly variable pathway inside the GoM (Figure 1), from a retracted position between the Yucatan Channel and the Florida Straits, to an extended position reaching the Northern GoM, before turning southeastward toward the Florida Straits, where it becomes the Florida Current. When it is highly extended, the LC eventually closes its clockwise circulation to form a large, anticyclonic eddy, called LC Eddy or ring, which then drifts westward inside the GoM. One or several temporary detachments are often observed before the final separation of a LC Eddy (Schmitz, 2005). The extended LC or a newly formed LC Eddy can directly interact with the MR plume and entrain a portion of it offshore (Walker et al., 1996; Schiller et al., 2011). The LC dynamics are also associated with the presence of smaller, cyclonic eddies at the edge of the LC front. These LC frontal eddies (LCFEs) interact with the current and play a dominant role in the LC dynamics, in particular the LC Eddy detachments and separation (Schmitz, 2005; Le Hénaff et al., 2012a, 2014; Donohue et al., 2015). When the LC is extended far to the north, these LCFEs can also interact with the MR plume. In particular, the proximity of an LCFE to the LC, or to a newly formed LC Eddy, is able to enhance the offshore export of MR waters (Walker et al., 1996, 2005; Morey et al., 2003b; Schiller et al., 2011; Androulidakis and Kourafalou, 2013, Schiller and Kourafalou, 2014). Independent from the LC frontal dynamics, the Northern GoM continental shelf slope presents a rich eddy activity, marked by the presence of both cyclonic and anticyclonic eddies that may interact with the MR plume (Hamilton, 1992; Hamilton et al., 2002; Schiller et al., 2011). Such mesoscale eddies played a key role during the Deepwater Horizon oil spill of 2010, during which a pair of anticyclonic and cyclonic eddies entrained part of the oil that was located southeast of the Mississippi Delta

southward toward the LC, which raised major concern that large of quantities of oil would be entrained toward the Florida Keys (Walker et al., 2011). Finally, the extension of the MR waters in the Northern GoM is favored in spring and summer by the intense stratification, due to the seasonal surface warming. The low mixing induced by this stratification allows the MR waters to extend on long distances (Ortner et al., 1995; Androulidakis and Kourafalou, 2013).

In this article, we investigate an episode of MR water export offshore the Mississippi Delta area that reached South Florida in the summer of 2014. This episode is well documented by *in situ* data, as the 3rd observation campaign of the Pulley Ridge research project[1] was taking place in the southern edge of the WFS at the time the MR plume reached that area. The Pulley Ridge research project aims at characterizing the mesophotic reef population in the area of Pulley Ridge and the Dry Tortugas, at the entrance of the Florida Straits (see Figure 6), and at investigating its potential to populate shallower reefs along the Florida Keys, i.e., in the direction of the main Loop Current/Florida Current oceanic system flow. This event provided an observational platform of upstream connectivity between these ecologically fragile South Florida coral reef systems and the nutrient-rich MR plume.

The scientific questions we want to address in this article are focused on the MR plume dynamics and the connectivity between the Mississippi Delta and remote South Florida coral reef systems. We focus on specific aspects of the related processes that have not been explored in the past and seek to answer the following questions:

- Can large quantities of waters of Mississippi origin reach South Florida coastal and reef areas during periods of low MR discharge?

[1] "Understanding Coral Ecosystem Connectivity in the Gulf of Mexico from Pulley Ridge to the Florida Keys" (http://www.coastalscience.noaa.gov/projects/detail?key=63).

- Can MR waters reach the Florida Straits following an alternative route to the common pathway along the Loop Current in the deep Gulf?
- What processes led to the inshore advection of MR waters upon their arrival to the Florida Straits in Summer 2014?

To answer these questions, we have developed a comprehensive, high-resolution regional hydrodynamic numerical model, able to reproduce both coastal and deep-sea flows in the dynamically and topographically complex GoM environment. The model employs the best available topography and high resolution/high frequency forcing fields (especially winds and river discharge). It also includes a dedicated scheme for representing the effect of river forcing. This approach, which consists in implementing a high-resolution regional model, nested in a global operational simulation and with improved physics and forcing, follows the recommendations drawn by the GODAE (Global Ocean Data Assimilation Experiment) OceanView (GoV) Coastal Ocean and Shelf Seas Task Team (COSS-TT) [2] international initiative for the development of Coastal Ocean Forecasting Systems (COFS, Kourafalou et al., 2015a,b). Finally, our model simulation incorporates observations through data assimilation to ensure the realism of important GoM features, especially dynamical processes such as the LC and associated eddies. The development of an efficient regional, data-assimilative simulation allows the investigation of past events, as is done here. It is also suitable for quantifying the performance of regional observing systems, another major activity within GoV (e.g., Oke et al., 2015), or for future forecasting capabilities. In the spirit of COFS, our simulation benefits from the seamless analysis capability developed from the global to the regional and coastal scales, which enables the detailed analysis of

[2] https://www.godae-oceanview.org/science/task-teams/coastal-ocean-and-shelf-seas-tt/

processes involved in coastal to offshore interactions in the GoM. The combined use of observations and model reanalysis outputs will allow us to draw the most complete picture of the 2014 MR waters export episode, and to investigate the processes affecting the MR plume. The observations and modeling tools used for this study are described in Section 2, together with an in-depth evaluation of the 2014 reanalysis simulation. We will then describe the 2014 episode in Section 3, and discuss it in Section 4. Conclusions will be presented in Section 5.

2. Methodology

2.1 Observations

2.1.1 In situ data

The summer 2014 MR water export episode was sampled during the third year summer Pulley Ridge cruise by the R/V *Walton Smith*, from August 13 to August 28. The R/V *Walton Smith* is equipped with a wide range of on-board instruments. Sampling of the seawater characteristics uses a continuous flow-through system that measures near-surface temperature, salinity, and fluorescence throughout the cruise. The ship is also equipped with two RD Instruments Acoustic Doppler Current Profilers (ADCP). Besides the continuous on-board measurements, the Deep Focus Plankton Imager (DPI, formerly In Situ Ichthyoplankton Imaging System, or ISIIS, Cowen and Guigand, 2008) was deployed to sample optical biological observations. In addition to the optical system, the DPI is equipped with environmental sensors including a CTD (SBE49, Seabird Electronics) and fluorometer (ECO FL (RT), Wetlabs chlorophyll-a fluorescence).

In addition to on-board data, we also use observations from the National Data Buoy Center (NDBC) managed by NOAA to describe the 2014 MR water export episode. We employ data from the NDBC mooring 42040, located off the Mississippi Delta (29°12'45"N 88°12'27"W), which is

equipped with various sensors measuring atmospheric quantities at 10 m above the sea, as well as ocean surface variables. We consider 10 m wind data from that mooring as the wind prevailing in the Mississippi Delta area.

Finally, other *in situ* data are also used to evaluate our high-resolution GoM reanalysis simulation. Three datasets are used for this purpose. The first one consists of ocean profiles from profiling floats present in 2014 in the Gulf of Mexico. These profiling floats measure the ocean temperature and salinity down to 2000 m. These data have been gathered in the NOAA World Ocean Database (WOD[3]). The second dataset is composed of the continuous measurements of temperature and salinity over the top 1000 m by a glider deployed in the GoM from August 20 to December 8 as part of the Global Temperature and Salinity Profile Programme (Sun et al., 2010). These glider measurements are also available in WOD. Finally, we also used the velocity data from the Global Drifter Program to evaluate our GoM reanalysis simulation. This program aims at providing measurements of near-surface ocean currents worldwide at 15 m depth. To do so, drifters are composed of a spherical buoy at the surface, connected to a nylon holey sock drogue (sea anchor) so that the drifting system tracks the water displacement at 15 m (Lumpkin and Pazos, 2007). The global drifter array data are managed and distributed by NOAA's Atlantic Oceanographic and Meteorological Laboratory (AOML[4]). In addition to the 6-hourly locations of the drifters, this dataset provides an estimate of the associated drifter velocity.

[3] www.nodc.noaa.gov
[4] www.aoml.noaa.gov/phod/dac/index.php

2.1.2 Remote sensing data

In order to complement the *in-situ* data, we also use remote sensing data. We use 3-day composite maps of chl-a derived from the National Aeronautics and Space Administration (NASA) Modis Aqua satellite data at the University of South Florida optical lab[5]. Chl-a maps are useful to qualitatively identify MR waters: the seasonal variations of net productivity in the Northern GoM are coherent with the dynamics of freshwater discharge (Justic et al., 1993). Nutrients, primarily nitrogen, supplied by the MR may stimulate phytoplankton production and raise the chl-a concentrations in the warm surface waters of the GoM (Rabalais et al., 2002). Chl-a maps have been widely used in the past to characterize MR waters advection (Walker et al., 1994; Kourafalou et al., 1996; Schiller et al., 2011; Androulidakis and Kourafalou, 2013).

In addition to chl-a maps, we also use altimetry observations from AVISO. We use the Maps of Absolute Dynamic Topography (MADT) products, which include the Sea Level Anomaly (SLA) estimated with altimeters in orbit, to which is added the Mean Dynamic Topography (MDT) that represents the time invariant part of the ocean topography, estimated by satellite and *in situ* observations. We use the AVISO data updated in 2014 (DUACS 2014), which uses the MDT CNES-CLS13 product. The MADT products have a resolution of 1/4° and are generated daily, although the orbits of the various altimeters in flight do not allow providing up to date information at each location of the ocean every day. The MADT products allow identifying the main dynamical features in the GoM, as the ocean surface topography is associated with currents through geostrophy. In particular, the LC is associated with a high sea level, and so are the anticyclonic eddies and LC Eddies, while cyclonic eddies are associated with a depression in sea level.

[5] http://optics.marine.usf.edu

Finally, we also employ Sea Surface Salinity (SSS) remote observations from the Soil Moisture and Ocean Salinity (SMOS) mission, started in 2010 and led by the European Space Agency (ESA). We use the SMOS Level 4a SSS products, at 0.5° resolution and estimated weekly. Another SSS dataset from remote sensing is available, from the Aquarius/Satélite de Aplicaciones Científicas (SAC)-D satellite data, launched in 2011 through collaboration between NASA and the Argentina Comisión Nacional de Actividades Espaciales (CONAE). Since Aquarius Level 3 data are available at 1° resolution only, compared to 0.5° for the SMOS data, they were found less appropriate for studying an episode of MR water export. We would like to stress here that these remotely sensed SSS products are still under evaluation. In particular, previous Aquarius and SMOS data, although they were found to be able to detect the spread of MR plume after the flooding episode of 2011, showed a significant difference in their mean values inside the GoM (Gierach et al., 2013). The difference in mean values is much smaller between these SSS products in 2014 (not shown), compared to what was found by Gierach et al. (2013).

2.2 Model Description

2.2.1 The HYCOM model

We use the Hybrid Coordinate Ocean Model (HYCOM) to simulate the dynamics in the GoM. HYCOM is a widely used Ocean General Circulation Model (OGCM) that solves the hydrostatic Navier–Stokes equations (primitive equations) applied to a thin layer of stratified ocean on a rotating Earth. HYCOM's distinguishing feature is a generalized vertical coordinate system that optimizes the distribution of vertical computational layers by making them isopycnal in stratified regions, terrain-following in shallow coastal regions, and isobaric in the unstratified mixed layer (Bleck, 2002). The ocean is described as a stack of shallow water layers of specified target density. The vertical coordinate layers are isopycnal when water of a specified target density

is present in a given water column, otherwise the layers transition to fixed-coordinates (pressure and terrain following sigma levels). The optimal configuration of the coordinate layers is generated every time step by a vertical grid generator. This arrangement makes HYCOM a good choice for application domains that include both the open ocean and shallow or unstratified regions (Winther and Evensen, 2006; Chassignet et al., 2006; Kourafalou et al., 2009; Halliwell et al., 2009).

The model solves the momentum equations for layer-integrated velocity, conservation equations for layer potential temperature and salinity, and a continuity equation for layer pressure thickness (mass conservation - the layer pressure thickness corresponds to layer thickness in pressure units and is used synonymously with layer thickness). The equations are horizontally discretized on an Arakawa C grid. The momentum equations are solved with a numerical scheme designed to conserve enstrophy (Sadourny, 1975). The computations are split into an external mode for the depth-averaged velocities and an internal baroclinic mode for the depth varying velocities. The barotropic equations are integrated forward in time with a forward-backward scheme, while a leapfrog scheme with an Asselin filter is used for the baroclinic equations (Asselin, 1972; Bleck and Smith, 1990). The tracer and continuity equations are solved with numerical schemes equipped with a Flux Corrected Transport (FCT) procedure to control Gibbs oscillations and to conserve the positive definiteness of the layer pressure thickness and the thermodynamic variables. The model is equipped with a suite of vertical mixing schemes (Halliwell, 2004); we use the K-Profile Parameterization (KPP, Large et al., 1994). Further, architectural details are given by Bleck and Smith (1990) and Bleck (2002), and details on model performance and validation are given by Chassignet et al. (2003). An exhaustive list of model capabilities and relevant technical details are also available in the HYCOM Users Manual[6] and the references therein.

[6] www.hycom.org

2.2.2 High-resolution Gulf of Mexico (GoM) HYCOM model set-up

Figure 1 presents the model domain, which covers the GoM and adjacent areas in the Caribbean Sea and the Atlantic Ocean. In order to represent in detail the export of MR waters in the GoM, our GoM-HYCOM reanalysis simulation has a 1/50° resolution (~2 km) and 32 vertical levels. This resolution is higher than other existing models covering the GoM. In addition to high resolution, the 1/50° GoM-HYCOM developed herein has details in coastal physics that are missing in other GoM models. In particular, it is optimized to realistically represent river plume dynamics, especially the development and evolution of the MR plume. The high-resolution set-up for the model developed herein has been adapted from the HYCOM implementation in the Northern GoM (NGOM) domain to study the local MR dynamics. NGoM-HYCOM has proven efficient in representing the intense MR variability and the various manifestations of its extension, including the episodes of offshore transport (Schiller et al., 2011; Schiller and Kourafalou, 2014; Androulidakis and Kourafalou, 2013). In particular, as in the NGOM simulation, the 1/50° GoM-HYCOM forcing includes realistic daily river forcing from 15 major rivers in the U.S. part of the domain, obtained through the U.S. Geological Survey (USGS), while additional small rivers are represented by their monthly climatology. Freshwater sources from rivers are prescribed following the updated parameterization by Schiller and Kourafalou (2010), which includes both salt and momentum fluxes due to the river discharge and allows a choice of distributing this freshwater discharge below the surface near the river mouth (here, a 5 m downward penetration is imposed, at 3 major discharge points around the MR Delta). There is no relaxation of salinity in the interior of the domain. The model high resolution is supported by a recently developed 1/50° resolution bathymetry dataset, based on merging 3 datasets of bottom topography and coastlines. The model is forced at the surface by the NAVy Global Environmental Model (NAVGEM, 0.5° resolution, every 3 hours). The surface forcing includes 10 m wind speed and wind stress, precipitation, short

and long wave surface radiations, air temperature and water vapor mixing ratio. Surface forcing fields affect the surface of the ocean model through bulk formulae. At the external boundaries the model fields are handled differently for the external mode, which is radiated through Flather-like conditions (Oey and Chen, 1992), and the internal mode, which is relaxed toward the larger scale forcing boundary conditions on a 21-grid point (~40 km) buffer zone. The regional model is nested at the open boundaries in the operational NRL global HYCOM simulation, at a daily rate. A no-slip condition is applied along the solid boundaries. A seamless transition is thus ensured from the global to the regional scale, which is particularly important for the realism of the oceanic currents entering and exiting from the GoM domain. The model is run from January 1 to December 31, 2014.

2.2.3 GoM-HYCOM data assimilation

In order to analyze the sequence of events that allowed the transport of MR waters from the Northern GoM to the south part of the WFS, our 1/50° GoM-HYCOM reanalysis simulation needs to be realistic and thus needs to assimilate observations. This is done through sequential data assimilation based on the Kalman approach, using an Ensemble Optimal Interpolation (EnOI) filter (e.g. Counillon and Bertino, 2009). The methodology and numerical tools are the same as those used for performing Observing System Simulation Experiments (OSSEs) in the GoM for testing the impact of airborne ocean profile surveys, using the HYCOM model at lower resolution (Halliwell et al., 2014; 2015). Details about the data assimilation filter can be found in the appendix of Halliwell et al. (2014). In our study, the model error covariance matrix used during the EnOI data assimilations step is estimated from an ensemble of model states from a 4-year long free-running simulation of the 1/50° GoM-HYCOM model, for the years 2010 to 2013. This free-running simulation has the same attributes as presented above, except that the atmospheric

forcing uses the Coupled Ocean Atmosphere Mesoscale Prediction System (COAMPS, 27 km resolution, every 3 hours). The COAMPS fields have higher spatial resolution but, unfortunately, they are not available after 2013. At each data assimilation step, once a day, the ensemble used for estimating the model error covariance is composed of model fields from a period of two months centered on the date of the data assimilation, with a 5-day interval, from each of the 4 years of the free-running simulation. Choosing model fields from the same period of the year for estimating the model error covariance matrix ensures that the error budget follow the seasonal evolution of the GoM. The free running simulation used to estimate the model error covariance matrix for data assimilation also provides the initial conditions, on January 1, of the 2014 reanalysis simulation. These initial conditions are thus not matching the actual, observed state of the GoM, especially in terms of dynamical features such as the LC. Data assimilation is to correct this mismatch in the first days or weeks of the simulation.

The observations assimilated in the 2014 GoM-HYCOM reanalysis are along-track altimetry and Sea Surface Temperature (SST) data. The along-track altimetry observations include the Absolute Dynamic Topography (ADT) from Jason-2, AltiKa, Cryosat-2, and, starting on April 4, 2014, HY-2. As for the MADT products, along-track ADT is the sum of MDT and SLA along the satellite tracks. As opposed to the mapped products, the along-track SLA is not interpolated. These along-track data, distributed by AVISO, are delayed-time, which generally are of better quality than the near-real time data. The presence of four altimeters in flight during the period of interest, in the spring and summer of 2014, should ensure a sufficient space and time coverage for resolving the mesoscale dynamics in the GoM (Pascual et al., 2006). Because the model mean Sea Surface Height (SSH) is arbitrary, the model SSH and altimetry ADT observations need to be adjusted in order to become comparable. Before assimilation, the observed along-track

data are corrected from the mean Absolute Dynamic Topography estimated in the entire GoM from the MADT data of that day. Similarly, the model SSH is corrected from the mean GoM SSH on the same day, before estimating the innovation during the data assimilation procedure. The observation errors for altimetry data have 3 cm amplitude, and are considered uncorrelated. The local observation radius for altimetry data is 210 km, which is the radius around each model grid point beyond which observations are ignored during the data assimilation procedure. Because the large-amplitude, high frequency barotropic processes affecting the continental shelf are not as well captured by altimetry data, altimetry observations at areas where the bathymetry is shallower than 150 m are also discarded from the data assimilation procedure. The SST data that are assimilated in our 1/50° GoM-HYCOM reanalysis simulation are from the U.S. Navy's Multichannel Sea Surface Temperature (MCSST) dataset, which is available on the U.S. Global Ocean Data Assimilation Experiment (USGODAE) server[7]. SST observation errors are considered uncorrelated, with amplitude of 0.3°C. The local observation radius for SST data is 100 km, and SST data are assimilated in areas where the bathymetry is deeper than 10 m.

2.2.4 Other data assimilative model simulations available in the GoM

In this paper, we evaluate the realism of our 1/50° GoM-HYCOM by comparison with observations, but also with two HYCOM simulations that are publicly available and have been used as community models in many studies. These simulations are run in near-real time by the U.S. Naval Research Laboratory (NRL, Stennis Space Center): the operational global (GLB) HYCOM (1/12° resolution; Chassignet et al., 2009) and the regional GoM-HYCOM (1/25° resolution; Prasad and Hogan, 2007). Both simulations are near-real time analysis products that are

[7] http://usgodae.org

disseminated through a THREDDS server at COAPS/Florida State University (through hycom.org). The NRL 1/25° GoM-HYCOM simulation is very relevant for comparison, as it covers the same domain as the model presented herein. Important differences in attributes are as follows: our implementation has double horizontal resolution (1/50°), additional vertical layers (32 vs. 27), and high frequency river forcing, compared with NRL's climatological forcing. The NRL 1/25° GoM-HYCOM simulations implements a relaxation of the model Sea Surface Salinity to climatological values, which is not the case in our 1/50° GoM-HYCOM simulation. It assimilates observations through a 3D-Var assimilation scheme (Cummings, 2005; Cummings and Smedstad, 2013). In addition to along-track altimetry and remotely sensed SST, the 1/25° GoM-HYCOM simulation also assimilates *in situ* SST as well as available vertical temperature and salinity profiles from eXpendable Bathythermographs (XBTs), ARGO floats and moored buoys. The suite of 1/25° GoM-HYCOM simulations performed at NRL has been long used in operational and research contexts. In particular, it supported many studies about the GoM circulation and its impact during the Deepwater Horizon oil spill in 2010 (e.g., Mezic et al., 2010; Valentine et al., 2012; Paris et al., 2012; Le Hénaff et al., 2012b). The 1/12° GLB-HYCOM uses the same data assimilation scheme as the 1/25° GoM-HYCOM, and assimilates the same types of observations (along track altimetry, SST, *in situ* profiles); like the /25° GoM-HYCOM, it implements a relaxation of the model Sea Surface Salinity to climatological values, unlike our 1/50° GoM-HYCOM simulation. The 1/12° GLB-HYCOM is considered one of the most robust operationally run global models, providing boundary conditions to several regional models around the world.

2.3 Evaluation of the High-Resolution Reanalysis Simulation

Before using our 1/50° GoM-HYCOM reanalysis to analyze the 2014 MR water export episode, we need to evaluate the realism of this simulation. This evaluation is done by comparing

ocean features from the simulation with observations. First, we compare the simulation outputs with independent observations that have not been assimilated in the simulation. As described in Section 2.1.1, these *in situ* data are composed of 15 m velocity estimates from the Global Drifter Program, of temperature and salinity sections from a glider deployed in the GoM from August to December 2014, and of temperature and salinity profiles down to 2000 m from profilers present in the GoM in 2014. This comparison with *in situ* data is complemented by a comparison of the SSS from our simulation with data from the SMOS space mission (Section 2.1.2). Figure 2a shows the location of the *in situ* observations used for evaluation, as well as the corresponding date for the glider measurements. Although there are some drifter measurements in the Western GoM, most of the drifter observations are located in the Eastern GoM down to Florida Straits, i.e. where the 2014 MR water export episode took place. The glider pathway is also limited to the Eastern GoM, over the continental shelf of the Northeastern GoM and the deep GoM where the LC extends. Finally, observations from the profiling floats are quite well spread throughout the whole GoM, although with limited observations in the Southwestern corner of the basin.

Figure 2b shows the monthly estimates, over the GoM, of the Root Mean Square Error (RMSE) of the 15 m velocity from our 1/50° GoM-HYCOM reanalysis with respect to drifter observations. The RMSE of the 15 m velocity from the near-real time NRL 1/25° GoM-HYCOM and 1/12° GLB-HYCOM simulations are also presented for comparison. Despite the fact that our 1/50° GoM-HYCOM reanalysis only assimilates surface data from remote sensing, the associated error level in 15 m velocity is comparable to the error from both NRL simulations, which also assimilate *in situ* data; error levels range from 0.1 to 0.4 $m.s^{-1}$.

We then compare the outputs from our 1/50° GoM-HYCOM reanalysis with the vertical section of temperature and salinity measured by the glider down to 1000 m. These sections are

presented on Figure 3, along with the temperature and salinity from our simulation at the same location and time. The simulation shows a realistic range of temperature at all levels. In addition, it shows realistic signature of dynamical features, in particular of cyclonic LC frontal eddies, detected around September 25 and in late October. These cyclonic eddies are associated with an upwelling of deep cold water that is well represented in the simulation during both periods. The salinity of the simulation is also very satisfying, and allows the identification of the main water masses of the Gulf of Mexico. In particular, the salinity maximum observed between 200 and 300 m in late August, September, and then in early October, is typical of the Subtropical Underwater, which is the signature of the LC. Despite a slightly weaker amplitude of the associated salinity maximum, this feature is well identified in our 1/50° GoM-HYCOM reanalysis. Below 600 m, salinity decreases in both the simulation and the observations, with a decrease in salinity slightly weaker in the simulation. Salinity vertical displacements, like temperature ones, are also the signature of dynamical features, and they are well represented in the simulation. The vertical temperature and salinity in the simulation thus show realistic vertical structure, in agreement with observed water masses and dynamical features.

This evaluation is extended to a quantitative comparison of the vertical temperature and salinity from our 1/50° GoM-HYCOM reanalysis with observations from vertical profiles down to 2000 m throughout 2014. Figure 4 shows the RMSE of the simulation in temperature and salinity. The corresponding RMSE for the NRL 1/25° GoM-HYCOM and 1/12° GLB-HYCOM simulations are presented for comparison. Figure 4a and 4b show the monthly RMSE, averaged over all levels in the upper 300 m, in temperature and salinity, respectively. The RMSE in temperature is between 1.2 °C and 1.8 °C for our 1/50° GoM-HYCOM reanalysis. This amplitude is comparable to both NRL simulations, although our 1/50° GoM-HYCOM reanalysis does not assimilate any *in situ*

profiles, which these models do. As for salinity, the RMSE from the 1/50° GoM-HYCOM reanalysis ranges between 0.15 and 0.3, comparable to the NRL 1/12° GLB-HYCOM simulation, whereas the RMSE from the NRL 1/25° GoM-HYCOM simulation is higher, ranging between 0.25 and 0.4. Figures 4c and 4d show the mean vertical profile of RMSE in temperature and salinity, respectively, for all three simulations. The RMSE in temperature of our 1/50° GoM-HYCOM reanalysis reaches a maximum between 100 and 200 m, before decreasing to 1300 m, below which it slightly increases. The RMSE in salinity is the largest close to the surface, with a secondary maximum of much smaller amplitude at 200 m. Then, the error level decreases down to 1300 m, below which it slightly increases. In both temperature and salinity, the error levels are comparable, in amplitude, with the performance of both NRL simulations, even though our simulation does not assimilate any *in situ* profiles. We expect that future assimilation of a comparable *in situ* data set as for the NRL simulations will further increase the accuracy of our high resolution GoM model.

The last comparison with independent data is performed by comparing our 1/50° GoM-HYCOM SSS with observations from the SMOS space mission. Figure 5a shows the RMSE in SSS between our 1/50° GoM-HYCOM reanalysis and SMOS data (see Section 2.1.2). It is about 0.7 from the beginning of the year until June, after which it increases in July and August. As will be seen later, this increase in the SSS RMSE in the 1/50° GoM-HYCOM simulation is presumably due to a limited salinity decrease during the MR waters export. The RMSE in SSS from the NRL 1/25° GoM-HYCOM simulation, which is initially close to the RMSE from the 1/50° GoM-HYCOM simulation, rapidly increases and reaches values of about 1.2 or 1.3 in the spring of 2014, before decreasing in July and August. The SSS RMSE of the 1/12° GLB-HYCOM tends to be close to the 1/50° GoM-HYCOM reanalysis. In August and September, the SSS RMSE from the three simulations tend to converge. They all decrease to about 0.7 at the end of 2014. The RMSE in SSS

with respect to SMOS data illustrates that the 1/50° GoM-HYCOM reanalysis generally performs well in representing the GoM surface salinity, although the RMSE with respect to observations increases during the MR export episode in summer. However, the RMSE in SSS of our 1/50° GoM-HYCOM reanalysis is lower than in the NRL 1/25° GoM-HYCOM simulation, and close to the 1/12° GLB-HYCOM simulation.

The evaluation of our 1/50° GoM-HYCOM reanalysis is complemented by a comparison between the simulated Sea Surface Height (SSH) with Maps of Absolute Dynamic Topography (MADT) from AVISO, although these quantities are not independent since our simulation assimilates along-track altimetry observations. However, this comparison is useful, since altimetry allows identifying dynamical features. It thus helps us evaluate how the simulation represents the main dynamical features of the GoM, in particular the LC and associated eddies. These features usually play a role in the advection of material (such as MR waters), in particular in the deep GoM. Figure 5b shows that the 1/50° GoM-HYCOM SSH RMSE ranges between 5 and 10 cm, after large initial errors drop thanks to data assimilation. For the whole year, with an average value of 7.5 cm, the error is significantly smaller than the SSH RMSE for the NRL 1/25° GoM-HYCOM simulation, which is between 7 and 14 cm with an average of 9.7 cm, and than the SSH RMSE for the 1/12° GLB-HYCOM, which is very close to the 1/25° GoM-HYCOM simulation. These low values indicate that our 1/50° GoM-HYCOM reanalysis is very satisfying in representing the large scale and mesoscale processes that are captured in the AVISO products.

3. Results

3.1 Detection of a Salinity Drop on the Southern Edge of the West Florida Shelf

Figure 6 shows the path of the R/V Walton Smith during the Pulley Ridge research cruise and the measured near-surface salinity, between August 13 and 18 (Figure 6a), and between August

18 and 28 (Figure 6b). The figures clearly show a significant drop in salinity in the whole study region between these two periods. This drop is evident on the time series of the near-surface salinity as detected by the on-board CTD (Figure 6c): on August 18, in less than an hour, the salinity drops from ~35.2 to ~32.3, and close to 32 a few hours later. Although the R/V Walton Smith sampled patches of higher salinity on August 19-21 and August 24-26, the near-surface salinity after August 18 was notably lower than before that date. Such a marked drop in salinity in the southern Florida area, where there are no local large rivers, suggests an episode of MR water export. It is comparable, in amplitude, to the salinity drop observed in the Florida Straits following the 1993 MR flood and the subsequent MR waters export episode (Ortner et al., 1995). Flooding conditions have indeed long been considered necessary for the export of MR waters toward the GoM interior and South Florida. Other favorable conditions for such export include winds on the Northern GoM shelf that support offshore removal of plume waters (ie. upwelling favorable winds), thermal stratification that enables even light winds to act on the upper layer low-salinity waters (summer conditions) and the LC system (including the Loop Current and associated eddy field) extending northward (Ortner et al., 1995; Schiller and Kourafalou, 2014).

The DPI instrument was deployed on three occasions during the same cruise, on August 22, 23, and 25, i.e., after the drop in salinity on August 18 (the locations are included on Figure 6b). The DPI instrument is originally designed for observing ichtyoplankton, based on optical measurements. To do so, the instrument is towed by the vessel, typically in a tow-yo pattern. This was done during the Pulley Ridge cruise, and the CTD sensors mounted on the DPI measured the temperature and salinity along these tow-yo patterns. Figure 7 shows sections of salinity during the three DPI deployments. The first two sections, which were measured one day apart in the same area over the continental shelf, show that the near-surface waters have salinity between 32 and 33,

and that this low-salinity water layer is ~10 m deep. The third section was taken slightly to the southeast of the first ones, around 83°W, on the shelf break. There, the layer of low-salinity water at the surface is 15 to 20 m deep, thicker than on the first two sections. Such thicknesses are comparable with the low-salinity layer of MR origin (10 to 20 m) observed near South Florida during the 1993 MR export episode (Ortner et al., 1995; Gilbert et al., 1996). These thickness values, and the amplitude of the salinity drop, indicate that the 2014 MR water export episode is a major one.

Based on previous events of MR waters export to the GoM interior, it is reasonable to expect that MR flooding, together with other favorable conditions (upwelling favorable winds in the Northern GoM, extended LC system), support the summer 2014 episode. Figure 8 shows that the values of the MR discharge in 2014 are actually very close to climatological values, and far from discharge values typical of flooding conditions (compare to the 2011 values in Figure 8, marking a strong MR flood; see also Androulidakis and Kourafalou, 2013). This indicates that, unlike other intense MR water export events, the 2014 MR case is not associated with a MR flood. However, it is a major event, with observed strong impacts all the way to the South Florida coral reefs. This makes this episode of MR waters export an original and unique study case.

3.2 Mississippi River Waters Export toward South Florida

Our 1/50° GoM-HYCOM reanalysis simulation was performed to investigate in detail the sequence of events that led to the export of MR waters from the Northern GoM to the Florida Straits and the south edge of the WFS. Figure 9 presents the Sea Surface Salinity (SSS) obtained from the 1/50° GoM-HYCOM reanalysis, at various dates from early June to early September. The deep GoM is usually associated with high salinity values around 36, while lower salinity is found

over the river influenced Northern GoM shelf. Initially, the low-salinity waters associated with the MR are contained on the Northern GoM shelf around the Mississippi Delta (Figure 9a). During the month of June, low-salinity waters extend to the east, along the Northern GoM coast, while part of the MR waters are also entrained offshore south and east of the Delta (Figure 9b-c). The eastward spreading of MR waters is associated with intense westerly and southwesterly winds between June 5 and June 25, i.e. upwelling favorable, which affect the Mississippi Delta region (Figure 10a). This process is quite common in spring and summer (Morey et al., 2003a,b; Schiller et al., 2011).

In early July, the spreading of MR waters along the coasts of the Northern GoM continues and reaches 85°W, at which point the low-salinity waters are directed southward (Figure 9d-e). A second eastward branch of low-salinity waters extends directly east of the Mississippi Delta and follows the slope of the Northern GoM shelf. In the Delta region, the eastward export is still favored by the southwesterly winds, which are dominant during most of July (except early in the month), associated with easterly wind bursts, all of which upwelling favorable (Figure 10b). This second eastward branch of low-salinity waters, south of the shelf, intensifies between middle and late July. The eastern tip of that branch extends southward and southeastward, following the edge of the continental shelf (Figure 9f-g), while a LC Eddy that detached in early July is located just south of the Mississippi Delta. LC Eddies approaching the Delta usually limit the westward extend of the MR plume and favor the eastward and offshore advection of MR waters, due to their anticyclonic circulation (Walker et al., 1996; Schiller et al., 2011). Such offshore export is visible in July, with a filament of low salinity clearly following the edge of the LC Eddy to the south (Figure 9d-h).

The situation seen in late July prevails in early August, with the main branch of low-salinity waters extending eastward from the Mississippi Delta, then southeastward along the WFS (Figure 9h). A large portion of these waters is removed offshore, where they are further entrained along

the LC, while a portion of the MR waters continues following the edge of the WFS southward (Figure 9i). This shelf route is consistent with a low-salinity water export pathway described in the model study by He and Weisberg (2002). The LC Eddy, which was able to entrain low-salinity waters from late July to early August, reattaches to the main LC front by mid-August, enabling the southward export of low-salinity waters toward the Florida Straits (Figure 9i-j). Between middle and late August, the plume of low-salinity waters reaches the Florida Straits and is entrained around a small, cyclonic LCFE located at the southwest corner of the WFS, at about (84°W; 24°N). More to the North, low-salinity waters keep being advected eastward, then southward along the LC during most of August. In the Mississippi Delta area, this entrainment is still favored by dominant westerly winds from August 5 to August 22 (Figure 10c).

The episode of MR waters export appears to decrease in early September. On September 1, the SSS signature of the low-salinity plume has overall decreased in the GoM (Figure 9k). As the wind in the Mississippi Delta area reverses to easterly wind, the patch of low-salinity waters in the Northern GoM retreats to the shelf, even though filaments of low-salinity waters are still entrained offshore (Figure 9k-l). This overall decrease in the signature of the MR plume in the GoM, associated with the interruption of the eastward entrainment of MR waters in the Northern GoM, marks the end of this extensive MR water export episode, which started in June.

3.3 Transfer of Low-Salinity Waters from the Deep GoM onto the Southern West Florida Shelf

We use the 1/50° GoM-HYCOM reanalysis to analyze how the branch of MR waters, which is offshore when it reaches the Florida Straits, is advected onto the continental shelf, where it was observed. Figure 11 shows the simulated SSS and surface currents over a subset of the model domain centered on the Florida Keys and the southern corner of the WFS, at various dates in August

and early September. On August 10, fresher waters associated with the MR water export are about to reach the Florida Straits. The LCFE located at the southwestern corner of the WFS is visible in surface currents, as well as the intense Florida Current that flows eastward, then northward along the coasts of Florida. Meandering of the Florida Current between Florida, Cuba and the Bahamas, associated with the presence of LCFEs is common (Kourafalou and Kang, 2012). On August 19, the filament of fresher waters visible on August 10 has been advected further into the Florida Straits. In particular, the cyclonic currents associated with the LCFE entrain surface waters toward the shelf, in the area where the low-salinity waters have first been observed by the R/V *Walton Smith* surveys. On August 26, the filament of fresh waters has kept advancing eastward into the Florida Straits, advected along the Florida Current, while the surface currents indicate shoreward currents along most of the Florida Keys. These currents are still visible on September 2, at which date a larger portion of the fresher waters has been advected onto the shelf, along the Florida Keys, as well as over the Dry Tortugas and in the Pulley Ridge area. The vast majority of the south Florida coral reefs is thus encompassed by an atypical mass of low-salinity (and also nutrient-rich) waters, with possible implications on water quality.

Figure 12 shows the surface winds from NAVGEM at the same dates. The NAVGEM model assimilates atmospheric observations, and as such presents a realistic wind field. For example, time series of winds at the MR Delta mooring site are almost identical to NAVGEM fields, as mooring data are assimilated in the atmospheric model (not shown). NAVGEM indicates that the winds in the mid-August to early September period are predominantly easterly or northeasterly winds along the Keys, i.e., downwelling favorable. This induces Ekman transport toward the shelf, which explains episodes of onshore transport along the Florida Keys, as seen on August 26 in the northern part of the Florida Keys, and on September 2. This transport increases

as winds intensify at the end of August and in early September: on September 2, the low-salinity waters extend far into the Florida Bay (north of the Florida Keys). The advection of MR waters from the deep GoM to the continental shelf, first over the narrow Florida Keys shelf and then the broader WFS, is thus favored by two processes: the cyclonic LCFE located at the southern corner of the WFS, and the intense easterly to northeasterly winds prevailing in the Florida Straits from mid-August to early September.

4. Discussion

We use remotely sensed chl-a images to evaluate how our 1/50° GoM-HYCOM reanalysis simulation represents the MR water export pathways in the GoM, since MR waters are associated with higher productivity visible in ocean color. Figure 13 presents 3-day composites of chl-a in the eastern GoM in spring and summer of 2014, at the same dates as Figure 9.

The reanalysis simulation reproduces well the initial eastward export of MR waters along the coasts of the Northern GoM until early July (Figures 9a-d and 13a-d), as well as the second eastward branch of low-salinity waters, directly east of the Mississippi Delta, in middle and late July (Figure 9e-f and 13e-f). The reanalysis simulation captures the reattachment of the LC Eddy in early August and its effect on the southward export of MR waters (Figure 13h-i). In both the simulation and the observations, the MR waters first move eastward, then southward along the WFS edge in July and August. Then they are eventually advected to the deep GoM and southward along the LC, before being advected around a LCFE located in the southwest corner of the WFS (Figure 13i-j). At the end of the export episode, in early September, the MR waters retreat on the shelf around the Mississippi Delta. The reanalysis simulation captures the decrease in the intensity

of the signature of the MR plume in the GoM, associated with the drastic diminution in the export of low-salinity waters from the Northern GoM.

We also analyze the performance of the 1/50° GoM-HYCOM reanalysis in terms of SSH, compared with the AVISO observation products. Figures 14 and 15 present the SSH from the reanalysis, and the observed MADT, respectively, at the same dates during the study period as on Figures 9 and 13. As expected from the assimilation of altimetric data, which have a major impact on ocean dynamics, the reanalysis simulation is able to represent the evolution of the LC, which is the dominant current in the GoM. In particular, the timing of the LC Eddy detachment between June 29 and July 5, as well as its reattachment between August 7 and 16, are captured by the reanalysis (Figures 14c-d, 15c-d, 14h-i, 15h-i). In addition, the reanalysis simulation realistically represents the eastward extension of the detached LC Eddy, which reaches the north of the WFS between mid-July and mid-August (Figures 14e-h, 15e-h). This eddy is relatively unusual, elongated far eastward, over the De Soto canyon (MAFLA shelf break). This orientation contributes to the eastward advection of MR waters, then to their southward advection along the WFS shelf break, with a secondary branch along the LC front. The export pathway along the LC is usually the main pathway, as seen in previous MR waters export events of 1993, 2004 and 2011 (Ortner et al., 1995; Hu et al., 2005; Schiller and Kourafalou, 2014; Androulidakis and Kourafalou, 2013). As seen in the observed chl-a (Figure 13), as well as the reanalysis SSS (Figure 9), the northern edge of this peculiar, elongated LC Eddy supports the eastward advection of low-salinity waters east of the Mississippi Delta, which forms the main branch of MR water export, south of the initial eastward propagation of MR waters along the coasts of the Northern GoM in June. However, although the SSH in the reanalysis tends to increase along the edge of the WFS between late July and mid-August, this increase is not as marked as in the observed MADT. This lower sea

level in the simulation explains why the low-salinity waters that were first advected eastward from the Mississippi Delta do not extend as far south as observed along the WFS. In particular, the LCFE located around (86°W; 27°N) on August 16 is more pronounced in the reanalysis, and it tends to advect low-salinity waters located on the WFS edge toward the deep GoM (Figure 14i), whereas in the observations MR waters keep being advected southward along the WFS edge, before being entrained to the deep GoM further south. Finally, the 1/50° GoM-HYCOM reanalysis captures well the LCFE located at the southwestern corner of the WFS in mid-August, around which the plume of low-salinity waters of MR origin is entrained (Figures 14i-k, 15i-k).

Based on qualitative comparisons with satellite data, the 1/50° GoM-HYCOM reanalysis was found able to capture the main dynamical features that allowed the export of MR waters from the Northern GoM toward the Florida Straits. These features include an initial branch of low-salinity along the Northern GoM coasts, followed by a second eastward branch in July and August that initially follows the edge of an elongated LC Eddy, before going southward along the edge of the WFS. The riverine waters are then advected to the deep GoM, where they are finally entrained along the LC. Such a pathway of MR waters, following the edge of the continental shelf of the Northern GoM and the WFS, before reaching the deep GoM at a location far from the Mississippi Delta area, has never been observed in previous episodes of MR water export. In episodes of 1993 (Ortner et al., 1995) and 2004 (Hu et al., 2005; Schiller and Kourafalou, 2014), the MR waters were advected along the elongated LC from locations much closer to the Mississippi Delta. In 2011, following a major MR flood (Figure 8), a filament of high chl-a of MR origin was also observed to be advected by the extended LC (see Androulidakis and Kourafalou, 2013, their Figure 16). The 2014 MR waters export toward the Florida Straits is thus unique, as it is not associated with MR flooding, and the southward pathway is unique. This “shelf route” is similar to a drifter

trajectory described by DiMarco et al. (2005, their Figure 2): drifter 06935, released near the edge of Texas-Louisiana shelf, was advected first eastward along the edge of the Northern GoM shelf, then southward along the edge of the WFS, before reaching the deep GoM at the south of the WFS. However, this pathway was not associated with MR waters at the time. It is also similar to the southward export route of low-salinity waters described in the model study by He and Weisberg et al. (2002), which had never been observed during a long-distance MR water export episode until 2014.

We now discuss how the 2014 MR waters export episode is represented in our 1/50° GoM-HYCOM reanalysis in terms of salinity amplitude. A first evaluation is done at the basin scale using remotely sensed SSS from SMOS (see Section 2.1.2). Figure 16 shows two weekly maps, in July and August, i.e. during the southward spreading of the MR waters, of the SSS measured by SMOS. The spatial and temporal resolutions of these datasets do not allow a precise characterization of the MR waters pathways compared to ocean color images, which is why the latter data were used to describe in detail the 2014 MR waters export episode. However, the SMOS dataset confirms how the low salinity water filament rapidly expands southward between July and August. In addition, it shows the signature of the tongue of low salinity waters extending southward, with SSS dropping to ~33, which is lower than the value of ~34.5 reached in our 1/50° GoM-HYCOM reanalysis (see Figure 9j). In the GoM interior, the SSS detected by SMOS appears to be larger than the one from our 1/50° GoM-HYCOM reanalysis at the dates shown on Figure 16, but the SSS variability there is quite large in SMOS (not shown). The limited drop in the surface salinity associated with MR waters in the 1/50° GoM-HYCOM reanalysis, compared to the observations from SMOS, is confirmed in the Florida Straits: there, the surface salinity from the

reanalysis drops from ~36 to ~35 (see Figure 11), whereas *in situ* data from the R/V Walton Smith show a more pronounced drop from ~35 to ~32 (see Figure 6).

The limited drop in surface salinity seen in the 1/50° GoM-HYCOM reanalysis suggests that the complex combination of dynamical processes affecting the plume, although overall satisfying in the reanalysis simulation, is still missing details or has even slight misplacements that control the far-field signature of the MR water pathways. We note that the study focuses on analyzing the observed processes, rather than a complete reproduction of observed values. However, the findings can lead to a discussion of possible discrepancies that played a role in the far-field quantitative differences between simulated and *in situ* values. For example, the simulated branch of low SSS on the edge of the WFS does not extend as far south as in the observations, before being entrained toward the deep GoM. This might have affected the timing with which some of the MR waters reached the Florida Straits. Indeed, the main filament of fresh waters advected into the Florida Straits in the reanalysis simulation reaches that area between August 19 and 26, whereas it was observed on August 18. The plume of MR waters in the 1/50° GoM-HYCOM reanalysis is sensitive to mesoscale features, and their exact location and size. In particular, the main branch of MR waters export to the east in the Northern GoM follows the edge of an LC Eddy that extends far eastward along the continental slope. Then, the rapid extension of that plume to the south, following the edge of the WFS, is associated with high sea level localized on the shelf slope, which is difficult to constrain in the assimilative model.

This stresses the need for altimetry data with high space and time resolution, able to improve the resolution of processes in the topographically complex GoM, especially at the interface between the deep GoM and the continental shelf. Future altimeters such as the Surface Water Ocean

Topography (SWOT) will improve the data coverage and precision, which should facilitate the constraining of small-scale features when observations are assimilated into models.

The assimilation of salinity observations should also improve the representation of river plumes in models. However, river plume signature is difficult to constrain through data assimilation, since temperature and salinity are closely related, and the assimilation scheme has to be specifically designed for treating river waters adequately. Data assimilation in the case of river waters is still an open field for research, and is not the focus of this paper. In addition, SSS data from remote sensing currently have too coarse spatial and temporal resolutions, and too large uncertainties to be used in data assimilation. Finally, there is currently a limited number of *in situ* salinity observations of the MR plume in the GoM to assimilate into models, and probably too few to efficiently constrain the plume signature and export branch dynamics.

5. Summary and Conclusions

In August 2014, surface waters of unusually low salinity (~32) were observed on the southern corner of the West Florida Shelf (WFS) and along the Florida Keys by the R/V *Walton Smith*, during a research cruise investigating potential biological connectivity between the deep Pulley Ridge and the shallow Florida Keys coral reefs. Despite the absence of major flooding in 2014, such salinity drop in the Florida Straits area indicates an intense export of low-salinity waters from the Mississippi River (MR). We set up a regional, high-resolution model over the Gulf of Mexico (GoM) and applied a careful parameterization of river plume dynamics to investigate this episode of MR waters export. We employed the HYCOM model at 1/50° resolution, nested in the 1/12° global (GLB) HYCOM, with high frequency atmospheric and river forcing, and data assimilation using a Kalman filter based on Ensemble Optimal Interpolation.

The 1/50° GoM-HYCOM reanalysis simulation used in this study compares well with independent observations in the GoM. In particular, it is able to represent the typical water masses of the basin. The error levels in the upper ocean temperature and salinity are of comparable amplitude as the errors achieved by reference NRL HYCOM GoM and GLB near-real time products, although our 1/50° GoM-HYCOM reanalysis simulation only assimilates altimetry and Sea Surface Temperature observations, whereas in NRL simulations *in situ* temperature and salinity profiles are assimilated in addition to surface observations. The error in near-surface currents is also satisfying, compared to velocity estimated by drifter data. The error in Sea Surface Salinity, estimated with respect to remotely sensed observations from SMOS, is on average lower than in the NRL 1/25° GoM-HYCOM simulation, and of comparable amplitude as in the GLB-HYCOM simulation. In addition, the error level in Sea Surface Height, estimated with respect to AVISO mapped products, is notably lower in our 1/50° GoM-HYCOM reanalysis, indicating that this simulation provides good estimates of the large scale and mesoscale dynamical features. These good performances qualify the 1/50° GoM reanalysis for further studies in the GoM.

The 1/50° GoM-HYCOM reanalysis adequately represented coastal to offshore interactions and helped investigate the role of several processes in advecting MR waters from the Mississippi Delta to the Florida Straits and South Florida's coastal environments. Starting in June, a plume of low-salinity waters was advected eastward along the Northern GoM coasts, before turning south. In July, it merges with a second eastward branch of MR waters that formed directly east of the Mississippi Delta. These branches were favored by dominant westerly and southwesterly winds in the Mississippi Delta area, as observed on *in situ* wind measurements. In addition to winds, the main eastward branch followed the edge of an anticyclonic Loop Current (LC) Eddy that detached from the LC in July. This particular LC Eddy was elongated far eastward along the edge of the

continental shelf, extending to the WFS. Following the gradient associated with high Sea Surface Height (SSH) on the edge of the WFS, the MR waters were advected southward, until entrained offshore to the deep GoM. There, the low-salinity waters were advected southward along the LC, until they were entrained along a cyclonic LC frontal eddy (LCFE) located at the southern corner of the WFS, before they finally reached the Florida Straits. The LCFE caused the advection of some of the MR waters onto the WFS, in the area of Pulley Ridge, where strong salinity gradients were observed. Further east, the dominant easterly-northeasterly winds in August and early September favored northward Ekman transport of the MR waters onto the shelf along the Florida Keys, where low-salinity waters were also observed.

The above sequence was corroborated by satellite observations and revealed a combination of several factors that led to the transport of low-salinity waters from the Mississippi Delta to the Florida Straits. In particular: the LC in northward extension, winds favoring eastward transport and the presence of an anticyclonic LC Eddy elongated toward the WFS. Eastward propagation of the MR plume over the Northern GoM shelf under the influence of westerly winds has been described in the past (Morey et al., 2003a,b; Schiller et al., 2011). Similarly, an LC Eddy or the LC are known to able to advect the MR plume offshore (Walker et al., 1996; Schiller et al., 2011). However, in the present case, the MR waters were not directly advected offshore in a southward route along the LC Eddy and the LC. They first extended far eastward along the Northern GoM continental shelf, reaching the WFS and following a southward route along the WFS shelf break, before finally being advected toward the deep GoM and along the LC, which eventually carried them toward the Florida Straits. This shelf route for low-salinity MR waters along the WFS is consistent with a pathway identified in the model study by He and Weisberg (2002). It is also consistent with the trajectory of a drifter deployed in 1992 (DiMarco et al., 2005). However, this is the first time that this route

between the Northern GoM and the Florida Straits is observed during an actual MR water export episode, as previous episodes of offshore export involved the advection of MR waters along the extended LC at locations much closer to the Mississippi Delta than seen in the present case (Ortner et al., 1995; Hu et al., 2005; Schiller and Kourafalou, 2014; Androulidakis and Kourafalou, 2013). This, in addition to the absence of flooding conditions, makes the 2014 MR waters export episode a unique one.

In the Florida Straits, the MR waters were advected onto the continental shelf by either a cyclonic eddy or the Ekman transport forced by easterly winds. These two processes are likely to influence the biological connectivity between the deep GoM and the Pulley Ridge and Florida Keys area, in the presence or absence of MR waters. The 2014 MR waters export episode thus reveals a variety of basin-wide connectivity processes, from the Northern GoM to the Florida Straits, and between the Florida Straits and the adjacent shelf, coastal and coral reef areas.

The 1/50° model reanalysis used for this study was found to generally compare well with observations of the GoM during the MR water export episode, with the exception that the salinity of the MR waters plume reaching the Florida Straits, although of realistic distribution, was not fresh enough. This is thought to be due to limitations in the representation of the dynamical processes affecting the advection of the MR waters away from the Mississippi Delta area and in particular the accuracy in the evolution of the complex and highly variable mesoscale circulation. The constraint of the exact location and intensity of mesoscale features is challenging in a topographically and dynamically complex area such as the GoM, and is the subject of active research in data assimilation. Future altimeters such as the Surface Water Ocean Topography (SWOT), which will provide high-resolution, two-dimensional sea level observations, should improve the representation of small-scale processes in assimilative simulations. In spite of these

limitations, the reanalysis simulation performed with the 1/50° GoM-HYCOM simulation developed here proves very useful to study the 2014 MR water export episode.

This high-resolution reanalysis illustrates the recent efforts made by the coastal and regional oceanography community to develop reanalysis products for studying specific events, which is highly encouraged within the Godae OceanView (GoV) Coastal Ocean and Shelf Seas Task Team (COSS-TT) group (Kourafalou et al., 2015a,b). In this study, a reanalysis simulation has been used, together with observations, to identify the complex interactions between various physical processes, which led to a long-distance connectivity episode in the GoM. High-resolution, regional nested modeling proved essential to the analysis and understanding of the key aspects of this episode, highlighting the need to accurately represent both coastal and deep processes, as well as their interaction.

Acknowledgments

This paper is a result of research funded by the National Oceanic and Atmospheric Administration (awards NA11NOS4780045, NA10OAR4320143 and NA12OAR4310073). M. Le Hénaff received partial support for this work from the base funds of the NOAA Atlantic Oceanographic and Meteorological Laboratory. The MODIS/Aqua satellite images of chlorophyll-a were provided by the Optical Oceanography Lab of USF/CMS (University of South Florida/College of Marine Science). The altimeter products were produced by Ssalto/Duacs and distributed by Aviso (http://www.aviso.altimetry.fr/duacs/), with support from CNES (Centre National d'Etudes Spatiales). MDT_CNES-CLS13 was produced by CLS (Collecte Localisation Satellites) Space Oceanography Division and distributed by Aviso (http://www.aviso.altimetry.fr/), with support from CNES. The SMOS L4 data were obtained from the Ocean Salinity Expertise

Center (CECOS) of the CNES-IFREMER Centre Aval de Traitemenent des Données SMOS (CATDS), at IFREMER, Plouzané (France). The authors would like to thank the crew and scientists on board the R/V Walton Smith during the Pulley Ridge project cruise (August 13-28, 2014), for collecting and providing *in situ* data; in particular, the water column salinity vertical profiles using DPI were provided by R. K. Cowen (Oregon State University). The bathymetry used in the 1/50° GoM-HYCOM reanalysis simulation was derived by P. Velissariou (COAPS, Florida State University). Finally, the authors wish to thank two anonymous reviewers for their constructive remarks.

References

Androulidakis YS, Kourafalou VH (2013) On the processes that influence the transport and fate of Mississippi water under flooding outflow conditions. Oc Dyn 63(2–3):143–164. doi 10.1007/s10236-0120587-8.

Asselin R (1972) Frequency filter for time integrations. Mon Weather Rev 100(6):487-490.

Bleck R (2002) An oceanic general circulation model framed in hybrid isopycnic-Cartesian coordinates. Ocean Modell 4:55–88. doi:10.1016/S1463-5003(01)00012-9.

Bleck R, Smith L (1990) A wind-driven isopycnic coordinate model of the north and equatorial Atlantic Ocean: 1. Model development and supporting experiments. J Geophys Res 95(C3):3273–3285. doi:10.1029/JC095iC03p03273.

Chassignet EP, Smith LT, Halliwell GR, Bleck R (2003) North Atlantic simulations with the Hybrid Coordinate Ocean Model (HYCOM): Impact of vertical coordinate choice, reference pressure and thermobaricity. J Phys Oceanogr 33:2504–2526. doi:10.1175/1520-0485(2003)033<2504:NASWTH>2.0.CO;2.

Chassignet EP, et al. (2006). Generalized vertical coordinates for eddy-resolving global and coastal ocean forecasts. Oceanography 19:118–129. doi:10.5670/oceanog.2006.95.

Chassignet EP, Hurlburt HE, Metzger EJ, Smedstad OM, Cummings J, Halliwell GR, Bleck R Baraille R, Wallcraft AJ, Lozano C, Tolman H, Srinivasan A, Hankin S, Cornillon P, Weisberg R, Barth A, He R, Werner C and Wilkin J (2009) U.S. GODAE: Global Ocean Prediction with the HYbrid Coordinate Ocean Model (HYCOM). Oceanography **22**: 48-59.

Counillon F, Bertino L (2009) High-resolution ensemble forecasting for the Gulf of Mexico eddies and fronts. Ocean Dyn 59:83–95.

Cowen RK, Guigand CM (2008) In situ ichthyoplankton imaging system (ISIIS): system design and preliminary results. Limnol Oceanogr Methods 6:126–132.

Cummings JA (2005) Operational multivariate ocean data assimilation. Q J Roy Meteor Soc 131:3583–3604.

Cummings JA, Smedstad OM (2013) Variational data assimilation for the global ocean. In Data Assimilation for Atmospheric. Oceanic and Hydrologic Applications (Vol. II) (pp. 303-343). Springer Berlin Heidelberg. doi:10.1007/978-3-642-35088-7_13.

DiMarco SF, Nowlin WD, Reid RO (2005) A statistical description of the velocity fields from upper ocean drifters in the Gulf of Mexico. Geophys Monogr Ser 161, edited by W. Sturges and A. Lugo-Fernandez, 101-109, AGU, Washington, D. C.

Donohue KA, Watts DR, Hamilton P, Leben R, Kennelly M, Lugo-Fernandez A (2015) Gulf of Mexico Loop Current Path Variability. Dyn Atmos Oceans. http://dx.doi.org/10.1016/j.dynatmoce.2015.12.003

Dowgiallo MJ ed. (1994) Coastal Oceanographic Effects of Summer 1993 Mississippi river Flooding. Special NOAA Report, March 1994, 74pp.

Gierach MM, Vazquez-Cuervo J, Lee T, Tsontos VM (2013) Aquarius and SMOS detect effects of an extreme Mississippi River flooding event in the Gulf of Mexico. Geophys Res Lett 40:5188–5193. doi:10.1002/grl.50995.

Gilbert PS, Lee TN, Podestá GP (1996) Transport of anomalous low-salinity waters from the Mississippi River flood of 1993 to the Straits of Florida. Cont Shelf Res 16(8):1065–1085.

Halliwell GR (2004) Evaluation of vertical coordinate and vertical mixing algorithms in the Hybrid Coordinate Ocean Model (HYCOM). Ocean Modell 7:285–322. doi:10.1016/j.ocemod.2003.10.002.

Halliwell GR, Barth A, Weisberg RH, Hogan PJ, Smedstad OM, Cummings J (2009) Impact of GODAE products on nested HYCOM simulations of the West Florida Shelf. Ocean Dyn 59:139–155. doi:10.1007/s10236-008-0173-2.

Halliwell GR, Srinivasan A, Kourafalou V, Yang H, Willey D, Le Hénaff M, Atlas R, (2014) Rigorous evaluation of a fraternal twin ocean OSSE system in the open Gulf of Mexico. J Atmos Ocean Technol 31 (1):105–130. http://dx.doi.org/10.1175/JTECH-D-13-00011.1.

Halliwell GR, Kourafalou V, Le Hénaff M., Shay LK, Atlas R (2015) OSSE impact analysis of airborne ocean surveys for improving upper-ocean dynamical and thermodynamical forecasts in the Gulf of Mexico. Prog Oc 130:32-46. doi:10.1016/j.pocean.2014.09.004.

Hamilton P (1992) Lower continental slope eddies in the central Gulf of Mexico. J Geophys Res 97(C2):2185–2200.

Hamilton P, Berger TJ, Johnson W (2002) On the structure and motions of cyclones in the northern Gulf of Mexico. J Geophys Res 107(C12), 3208. doi:10.1029/1999JC000270.

He R, Weisberg RH (2002) West Florida shelf circulation and temperature budget for the 1999 spring transition. Cont Shelf Res 22, 719-748.

Hu C, Nelson JR, Johns E, Chen Z, Weisberg RH, Müller-Karger FE (2005) Mississippi River water in the Florida Straits and in the Gulf Stream off Georgia in summer 2004. Geophys Res Lett 32, L14606. doi:10.1029/2005GL022942.

Justic D, Rabalais NN, Turner RE, Wiseman WJ Jr (1993) Seasonal coupling between riverborne nutrients, net productivity and hypoxia. Mar Pollut Bull 26:184–189.

Kourafalou VH, Lee TN, Oey LY, Wang JD (1996) The fate of river discharge on the continental shelf, 2: transport of coastal low salinity waters under realistic wind and tidal forcing. J Geophys Res 101(C2):3435–3455.

Kourafalou VH, Peng G, Kang H, Hogan PJ, Smedstadt OM, Weisberg RM, Baringer MO, Meinen CS (2009) Evaluation of global ocean data assimilation experiment products on South Florida nested simulations with the Hybrid Coordinate Ocean Model. Ocean Dyn 59:47–66. doi:10.1007/s10236-008-0160-7.

Kourafalou VH, Kang H (2012) Florida Current meandering and evolution of cyclonic eddies along the Florida Keys Reef Tract: are they inter-connected? J Geophys Res 117, C05028. doi:10.1029/2011JC007383.

Kourafalou VH, Androulidakis YS (2013) Influence of Mississippi River induced circulation on the Deepwater Horizon oil spill transport. J Geophys Res 118(8):3823–3842. doi: 10.1002/jgrc.20272.

Kourafalou VH, De Mey P, Le Hénaff M, Charria G, Edwards CA, He R, Herzfeld M, Pascual A, Stanev EV, Tintoré J, Usui N, Van Der Westhuysen AJ, Wilkin J, Zhu X (2015a) Coastal Ocean Forecasting: system integration and validation. J Oper Oceanogr. doi:10.1080/1755876X.2015.1022336.

Kourafalou VH, De Mey P, Staneva J, Ayoub N, Barth A, Chao Y, Cirano M, Fiechter J, Herzfeld M, Kurapov A, Moore AM, Oddo P, Pullen J, van der Westhuysen AJ, Weisberg RH (2015b) Coastal Ocean Forecasting: science foundation and user benefits. J Oper Oceanogr. doi:10.1080/1755876X.2015.1022348.

Large WG, McWilliams JC, Doney SC (1994) Oceanic vertical mixing: A review and a model with a nonlocal boundary layer parameterization. Rev Geophys 32:363–403, doi:10.1029/94RG01872.

-Le Hénaff M, Kourafalou VH, Morel Y, Srinivasan A (2012a) Simulating the dynamics and intensification of cyclonic loop current frontal eddies in the Gulf of Mexico. J Geophys Res 117(C2), C02034. doi:10.1029/2011JC007279.

Le Hénaff M, Kourafalou VH, Paris CB, Helgers J, Aman ZM, Hogan PJ, Srinivasan A (2012b) Surface Evolution of the Deepwater Horizon Oil Spill Patch: Combined Effects of Circulation and Wind-Induced Drift. Environ Sci Technol 46:7267–7273.

Le Hénaff M., Kourafalou VH, Dussurget R, Lumpkin R (2014) Cyclonic activity in the eastern Gulf of Mexico: Characterization from along-track altimetry and *in situ* drifter trajectories. Prog Oc. 120: 120-138.

Lumpkin R, Pazos M (2007) Measuring surface currents with Surface Velocity Program drifters: the instrument, its data, and some recent results. In: Griffa A et al. (Eds.), Lagrangian Analysis and Prediction of Coastal and Ocean Dynamics. Cambridge Univ. Press, Cambridge, UK, pp. 39–67.

Mezic I, Loire S, Vladimir A, Fonoberov A, Hogan P (2010) A new mixing diagnostic and Gulf oil spill movement. Science 330:486–489.

Morey SL, Martin PJ, O'Brien JJ, Wallcraft AA, Zavala- Hidalgo J (2003a) Export pathways for river discharged fresh water in the northern Gulf of Mexico. J Geophys Res 108(C10), 3303. doi:10.1029/2002JC001674.

Morey SL, Schroeder WW, O'Brien JJ, Zavala-Hidalgo J (2003b) The annual cycle of riverine influence in the eastern Gulf of Mexico basin. Geophys Res Lett 30(16), 1867. doi: 10.1029/2003GL017348.

Oey LY, Chen P (1992) A nested-grid ocean model: With application to the simulation of meanders and eddies in the Norwegian Coastal Current. J Geophys Res 97(C12):20,063–20,086, doi:10.1029/92JC01991.

Oke PR, Larnicol G, Jones EM, Kourafalou V, Sperrevik AK, Carse F, Tanajura CAS, Mourre B, Tonani M, Brassington GB, Le Hénaff M, Halliwell GR, Atlas R, Moore AM, Edwards CA, Martin MJ, Sellar AA, Alvarez A, De Mey P, Iskandarani M. 2015. Assessing the impact of observations on ocean forecasts and reanalyses: Part 2, Regional applications. J Oper Oceanogr. doi:10.1080/1755876X.2015.1022080.

Ortner PB, Lee TN, Milne PJ, Zika RG, Clarke ME, Podestá GP, Swart PK, Tester PA, Atkinson LP, Johnson WR (1995) Mississippi River flood waters that reached the Gulf Stream. J Geophys Res 100(C7):13595–13601.

Paris CB, Le Hénaff M, Aman ZM, Subramaniam A, Helgers J, Wang DP, Kourafalou, VH, Srinivasan A (2012) Evolution of the Macondo well blowout: simulating the effects of the circulation and synthetic dispersants on the subsea oil transport. Environ Sci Technol 46(24):13293–13302.

Pascual A, Faugère Y, Larnicol G, Le Traon PY (2006) Improved description of the ocean mesoscale variability by combining four satellite altimeters. Geophys Res Lett L0261, 1–4. http://dx.doi.org/10.1029/2005GL024633.

Prasad, T.G., P.J. Hogan (2007) Upper-ocean response to Hurricane Ivan in a $1/25^0$ nested Gulf of Mexico HYCOM, *J. Geophys. Res.*, 112, C04013, doi:10,129/2006JC003695.

Rabalais NN, Turner RE, Wiseman WJ Jr, Boesh DF (1991) A brief summary of hypoxia on the northern Gulf of Mexico continental shelf: 1985–1988. In: Tyson, R.V. and Pearson, T.H. (eds.). Modern and Ancient Continental Shelf Anoxia. London: Geological Society of London, Special Publication 58:35–47.

Rabalais NN, Turner RE, Wiseman WJ Jr (2002) Gulf of Mexico hypoxia, a.k.a. "the dead zone." Annu Rev Ecol Evol Syst 33:235–263. doi:10.1146/annurev.ecolsys.33.010802.150513.

Sadourny R (1975) The dynamics of finite-difference models of the shallow-water equations. J Atmos Sci 32(4):680-689.

Schiller RV, Kourafalou VH (2010) Modeling river plume dynamics with the hybrid coordinate ocean model. Ocean Modell 33(1–2):101–107.

Schiller RV, Kourafalou VH, Hogan P, Walker ND (2011) The dynamics of the Mississippi River plume: impact of topography, wind and offshore forcing on the fate of plume waters. J Geophys Res 116(C6), C06029. doi:10.1029/2010JC006883.

Schiller RV, Kourafalou VH (2014) Loop Current impact on the transport of Mississippi River waters. J Coastal Res 30(6):1287-1306.

Schmitz WJ (2005) Cyclones and westward propagation in the shedding of anticyclonic rings from the Loop Current, in Circulation in the Gulf of Mexico: Observations and Models, Geophys Monogr Ser 161, edited by W. Sturges and A. Lugo-Fernandez, 241–261, AGU, Washington, D. C.

Sun C et al. (2010) "The Data Management System for the Global Temperature and Salinity Profile Programme" in Proceedings of OceanObs.09: Sustained Ocean Observations and Information for Society (Vol. 2), Venice, Italy, 21-25 September 2009, Hall J, Harrison DE, Stammer D, Eds. ESA Publication WPP-306. doi:10.5270/OceanObs09.cwp.86.

Valentine DL, Mezic I, Macesic S, Crnjaric-Zic N, Ivic S, Hogan PJ, Fonoberov VA, Loire S (2012) Dynamic autoinoculation and the microbial ecology of a deep water hydrocarbon irruption. P Natl Acad Sci USA 109:20286–20291. doi:10.1073/pnas.1108820109.

Walker ND, Fardion GS, Rouse LJ, Biggs DC (1994) Circulation of Mississippi River water discharged into the northern Gulf of Mexico by the great flood of summer 1993. Eos Trans Am Geophys Union 75(36):409–415.

Walker ND (1996) Satellite assessment of Mississippi River plume variability: Causes and predictability. Remote Sens Environ 58:21–35. doi:10.1016/0034-4257(95)00259-6.

Walker ND, Huh OK, Rouse LJ Jr, Murray SP (1996) Evolution and structure of a coastal squirt off the Mississippi River delta: Northern Gulf of Mexico. J Geophys Res 101(C9):20643–20655.

Walker ND, Leben RR, Balasubramanian S (2005) Hurricane-forced upwelling and chlorophyll a enhancement within cold-core cyclones in the Gulf of Mexico. Geophys Res Lett 32(18), L18610. doi:10.1029/2005GL023716.

Walker ND, Pilley C, Raghunathan V, D'Sa E, Leben R, Hoffmann N, Brickley P, Coholan P, Sharma N, Graber H, Turner R (2011) Impacts of Loop Current frontal cyclonic eddies and wind forcing on the 2010 Gulf of Mexico oil spill. Geoph Monog Series, 195, 103–116.

Weisberg RH, He R, Liu Y, Virmani JI (2005) West Florida shelf circulation on synoptic, seasonal, and interannual time scales. Geophys Monogr Ser 161, edited by W. Sturges and A. Lugo-Fernandez, 325-347, AGU, Washington, D. C.

Winther NG, Evensen G (2006) A Hybrid Coordinate Ocean Model for shelf sea simulation. Ocean Modell 13:221–237. doi:10.1016/j.ocemod.2006.01.004.

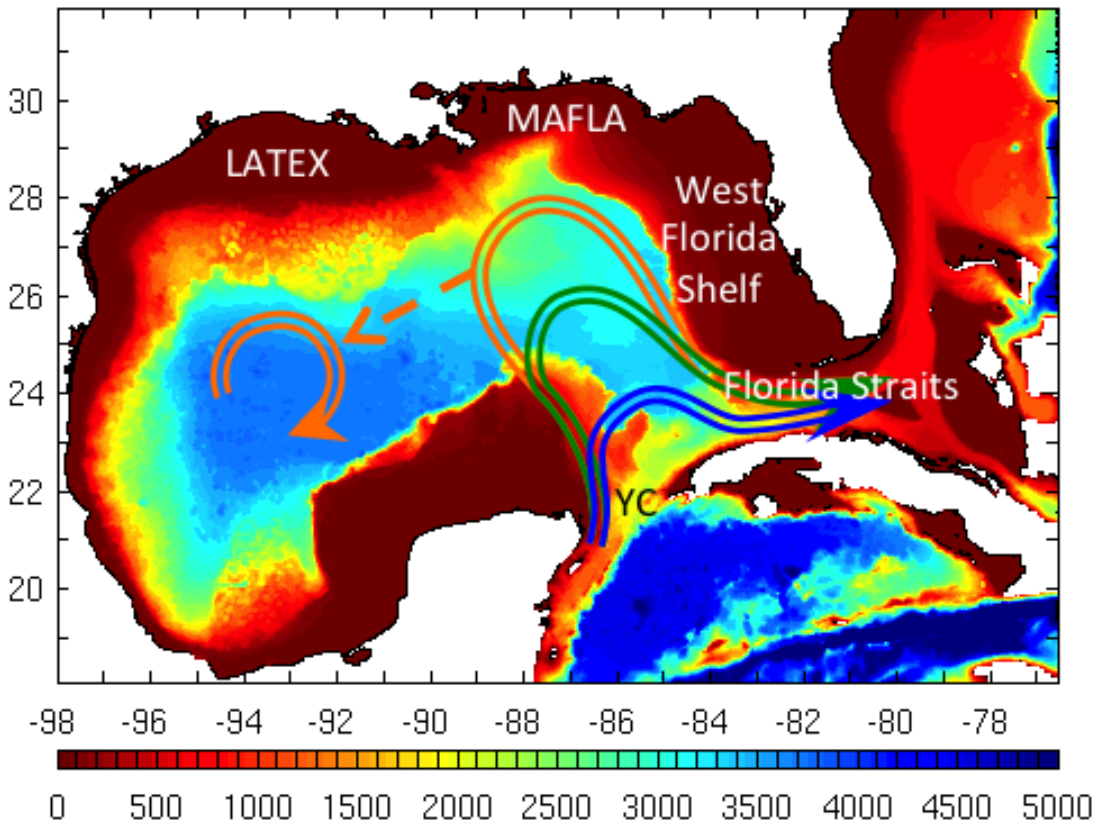

Figure 1: Topography of the Gulf of Mexico model domain (m). The colored arrows indicate various stages of the Loop Current (LC) extension: retracted, or port-to-port (blue), average extended position (green), fully extended with a LC Eddy shed (orange). Adapted from Le Hénaff et al. (2012a). Important bathymetric or geographic features are noted: the Louisiana-Texas (LATEX) shelf, the Mississippi-Alabama-Florida (MAFLA) shelf, the West Florida Shelf, the Florida Straits, and the Yucatan Channel (YC).

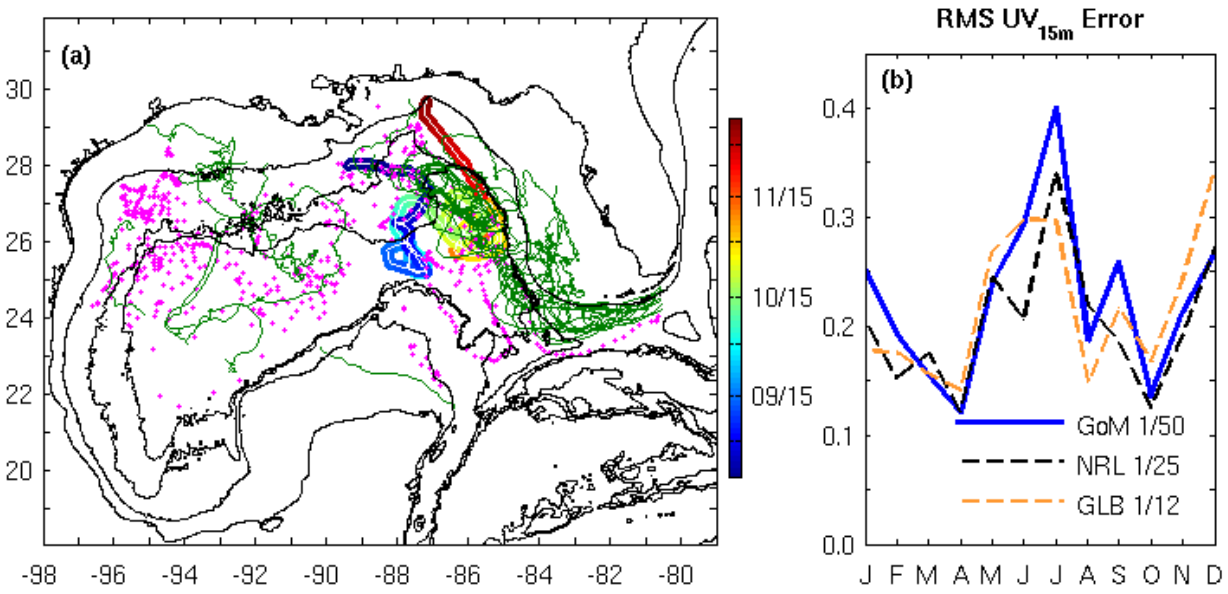

Figure 2: (a) Map of in situ measurements (green lines: drifter trajectories, magenta points: vertical temperature and salinity profiles); the colored line represents the glider pathway, with corresponding dates in the colorbar; (b) Monthly Root-Mean-Square Error ($m.s^{-1}$) between 15 m drifter velocity amplitude observations and: (blue line) the 1/50° GoM-HYCOM reanalysis simulation, (orange dashed line) the NRL 1/25° GoM-HYCOM simulation, and (black dashed line) the NRL 1/12° GLB-HYCOM simulation.

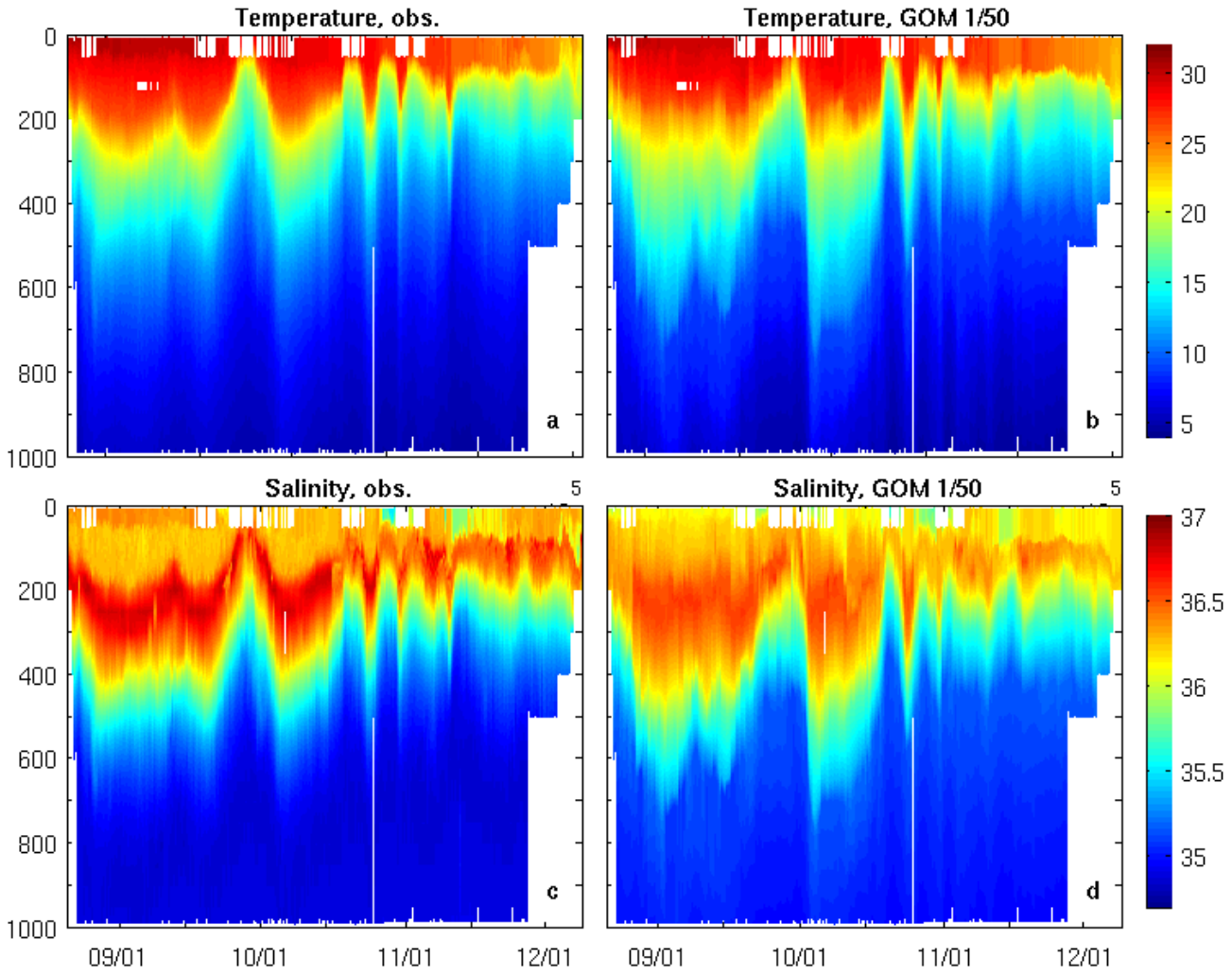

Figure 3: (a) Time-depth vertical section of temperature (°C) measured by a glider deployed in the GoM between August 20 and December 8; (b) same as (a), except the data are extracted from the 1/50° GoM-HYCOM reanalysis simulation; (c-d) same as (a-b), except for salinity.

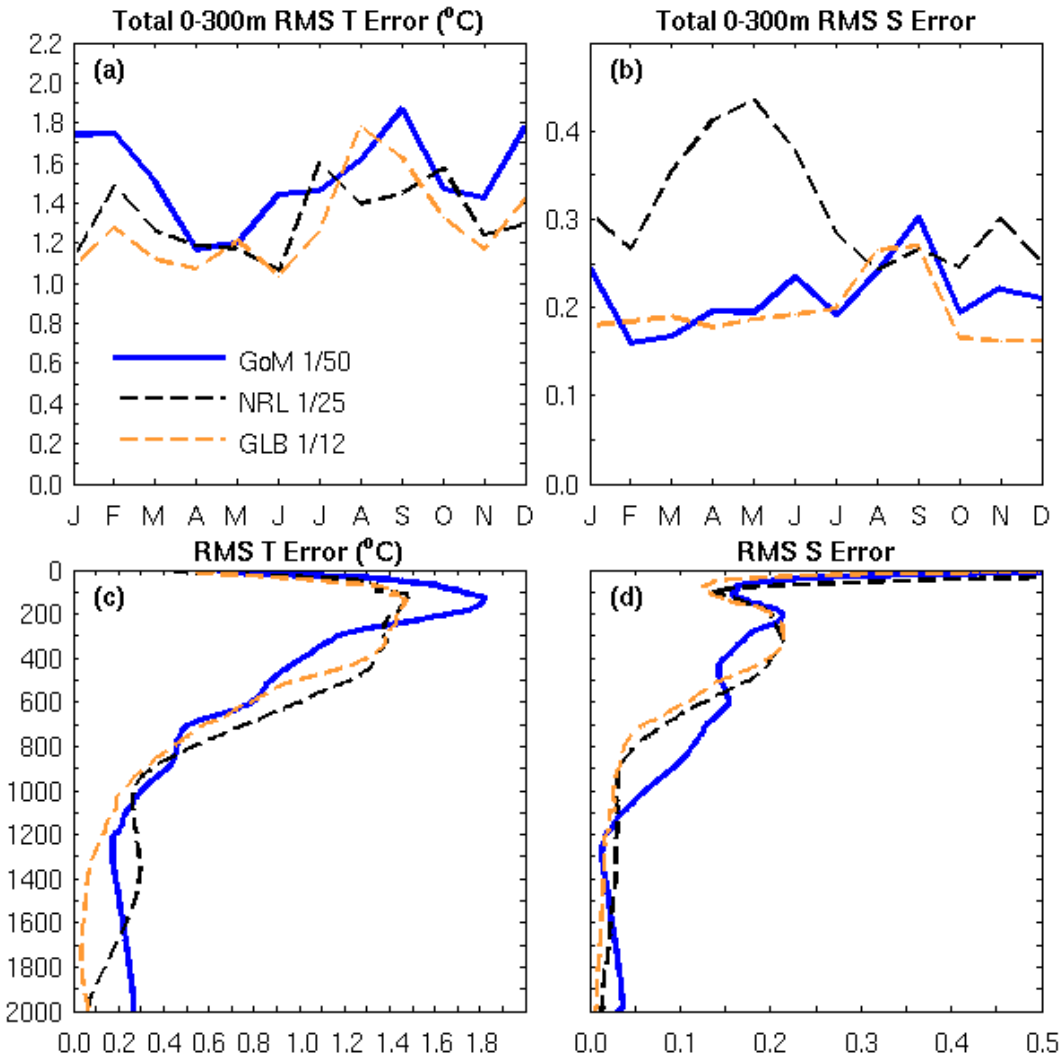

Figure 4: (a) Monthly Root-Mean Square Error (RMSE) in temperature (°C) estimated over the top 300 m between observations from profiles deployed in the GoM in 2014 and: (blue line) the 1/50° GoM-HYCOM reanalysis simulation, (orange dashed line) the NRL 1/25° GoM-HYCOM simulation, and (black dashed line) the NRL 1/25° GoM-HYCOM simulation; (b) same as (a) except for salinity; (c) vertical profile down to 2000 m of the 2014 mean RMSE in temperature (°C) for the same simulations; (d) same as (c) except for salinity.

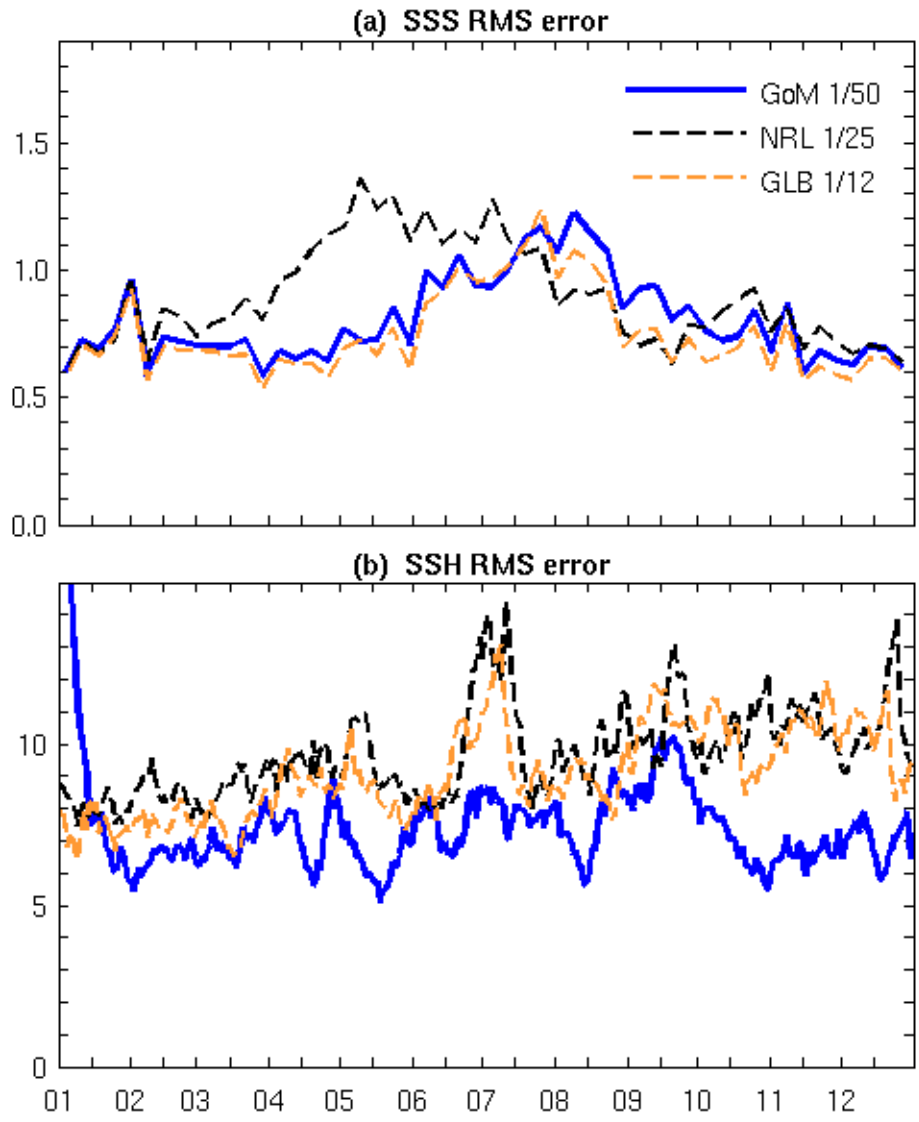

Figure 5: Time series of the Root Mean Square Error of (blue line) the 1/50° GoM-HYCOM reanalysis, (orange dashed line) the NRL 1/25° GoM-HYCOM simulation, and (black dashed line) the NRL 1/12° GLB-HYCOM simulation, in (a) Sea Surface Salinity with respect to weekly SMOS data, (b) Sea Surface Height with respect to daily AVISO MADT (cm). Numbers at the bottom indicate the first day of the respective months of 2014.

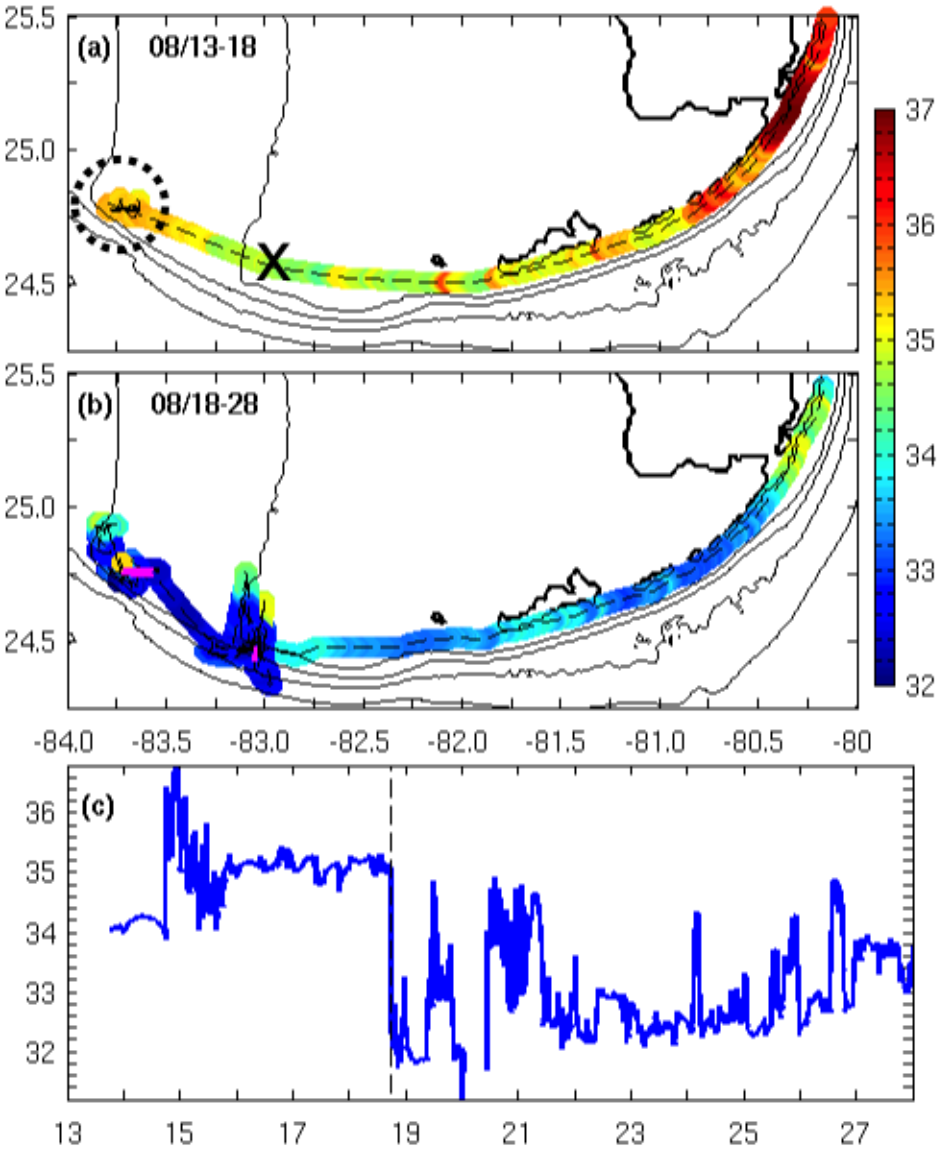

Figure 6: (a) Near surface Salinity measured on-board the R/V Walton Smith between August 13 and 18, 2014; (b) same as (a), for the August 18 to 28 period; the short magenta lines indicate the locations of DPI measurements: two zonal sections at approximately (83.7°W; 24.75°N) and one meridional section at approximately (83.1°W; 24.5°N); (c) time series of the observed near surface salinity during the full period August 13-28, 2014; the vertical black dotted line indicates the limit between measurements shown on panels (a) and (b). (a) The dotted circle marks the location of Pulley Ridge; the "x" symbol marks the Dry Tortugas; the Florida Keys island chain extends to the northeast. (a, b): the thin black lines indicate the isobaths at 50, 100, 200, and 500 m.

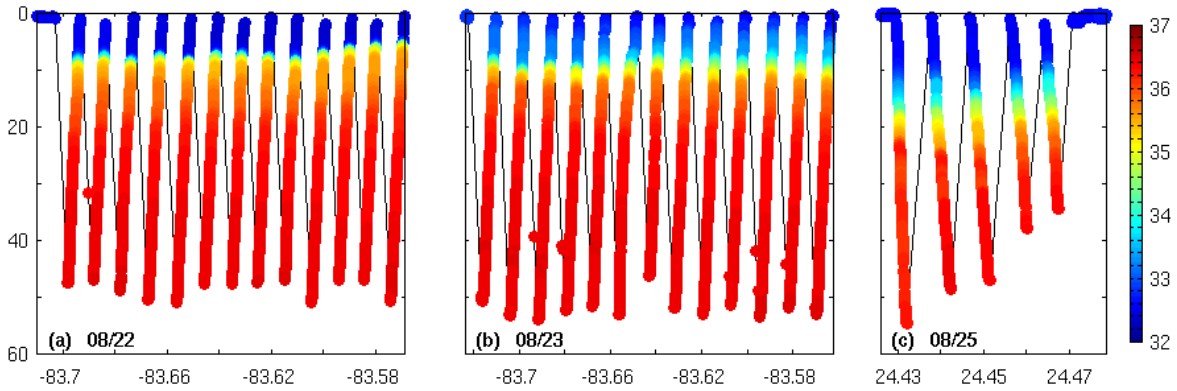

Figure 7: Vertical sections of the salinity observed using the DPI instrument towed by the R/V *Walton Smith*, on (a) August 22, (b) August 23, and (c) August 25, 2014. (a) and (b) are oriented eastward, while (c) is oriented northward. Because of the time delay for the pump that entrains the seawater to the CTD mounted on the DPI, only the salinity values from the ascending parts of the tow-yo pattern are plotted (the instrument moves from left to right in panels a and b, and from right to left in panel c).

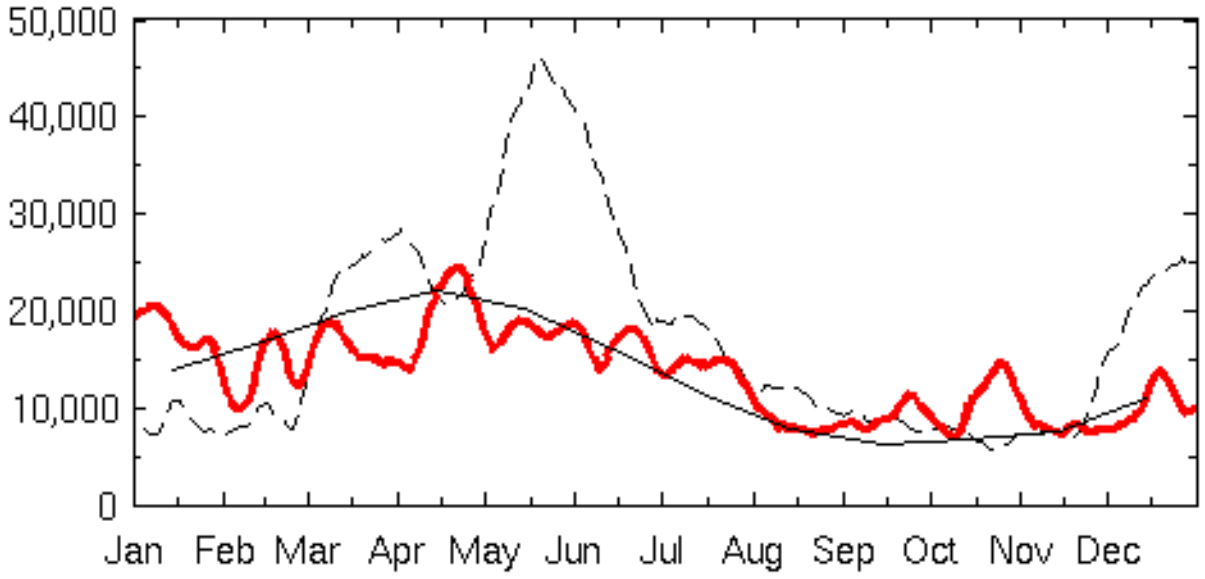

Figure 8: Time series of the Mississippi River discharge (m^3/s) in 2014 (red) and 2011 (dashed black). In black are the climatological values.

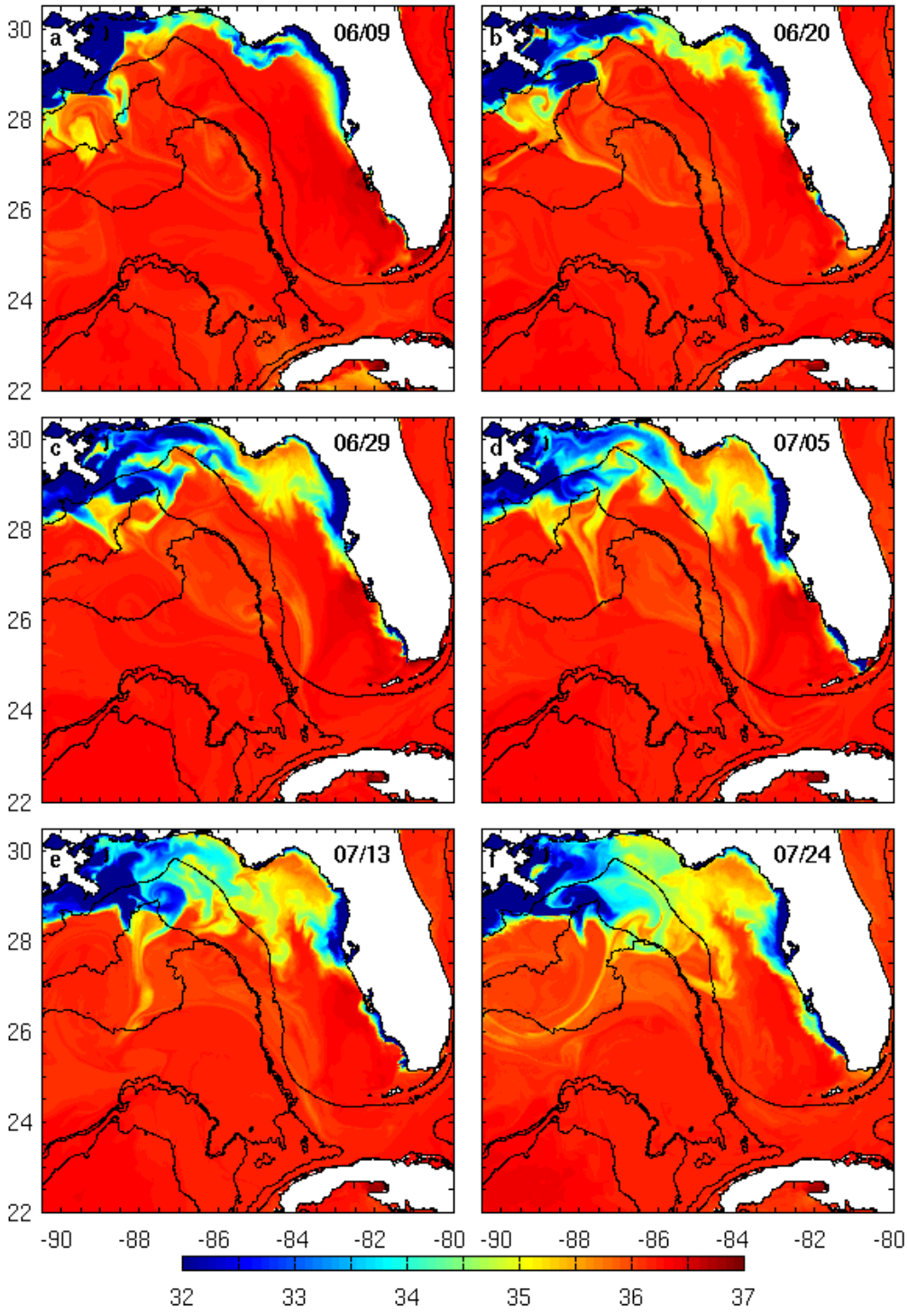

Figure 9: Snapshots of the 1/50° GoM-HYCOM reanalysis Sea Surface Salinity (zoom on the eastern GoM) on (a) June 9, (b) June 20, (c) June 29, (d) July 5, (e) July 13, and (f) July 24. Black lines represent the 200, 2000, and 3000 m isobaths.

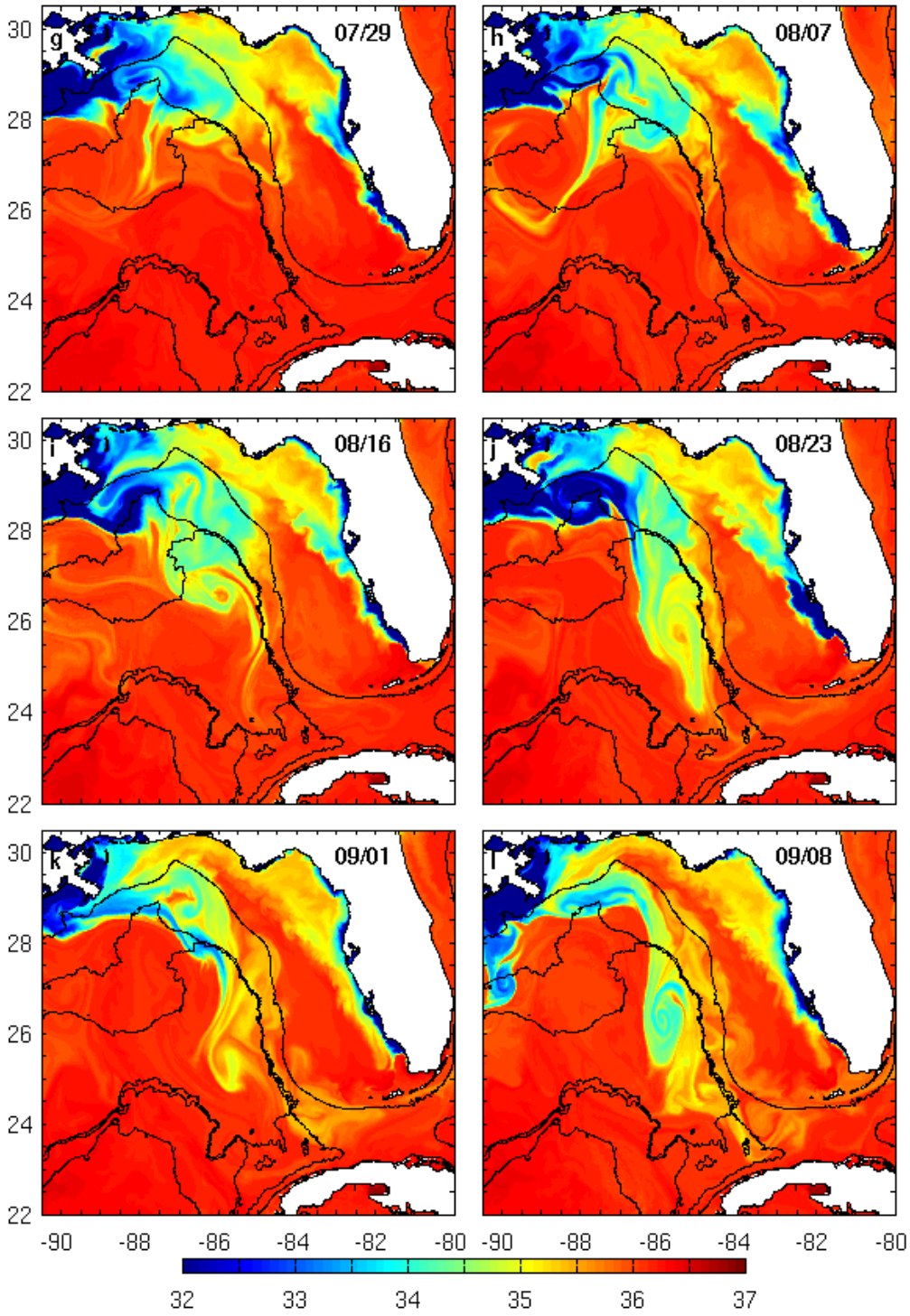

Figure 9 (continued): Snapshots of the 1/50° GoM-HYCOM reanalysis Sea Surface Salinity (zoom on the eastern GoM) on (g) July 29, (h) August 7, (i) August 16, (j) August 23, (k) September 1, and (l) September 8. Black lines represent the 200, 2000, and 3000 m isobaths.

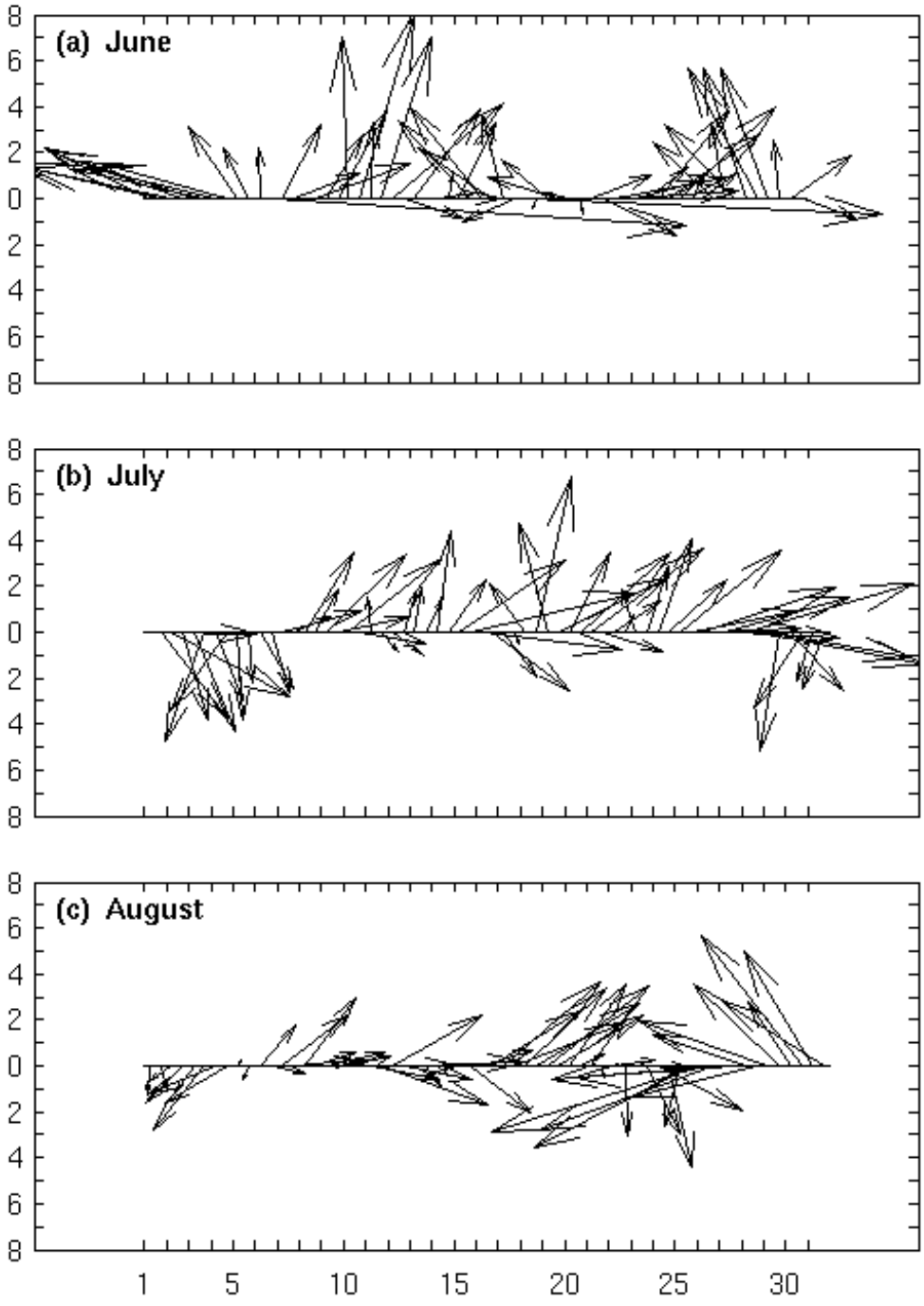

Figure 10: Time evolution of 12-hourly winds ($m.s^{-1}$) observed at the National Data Buoy Center (NDBC) mooring 42040, located off the Mississippi Delta (29°12'45"N 88°12'27"W) during (a) June, (b) July, and (c) August, 2014.

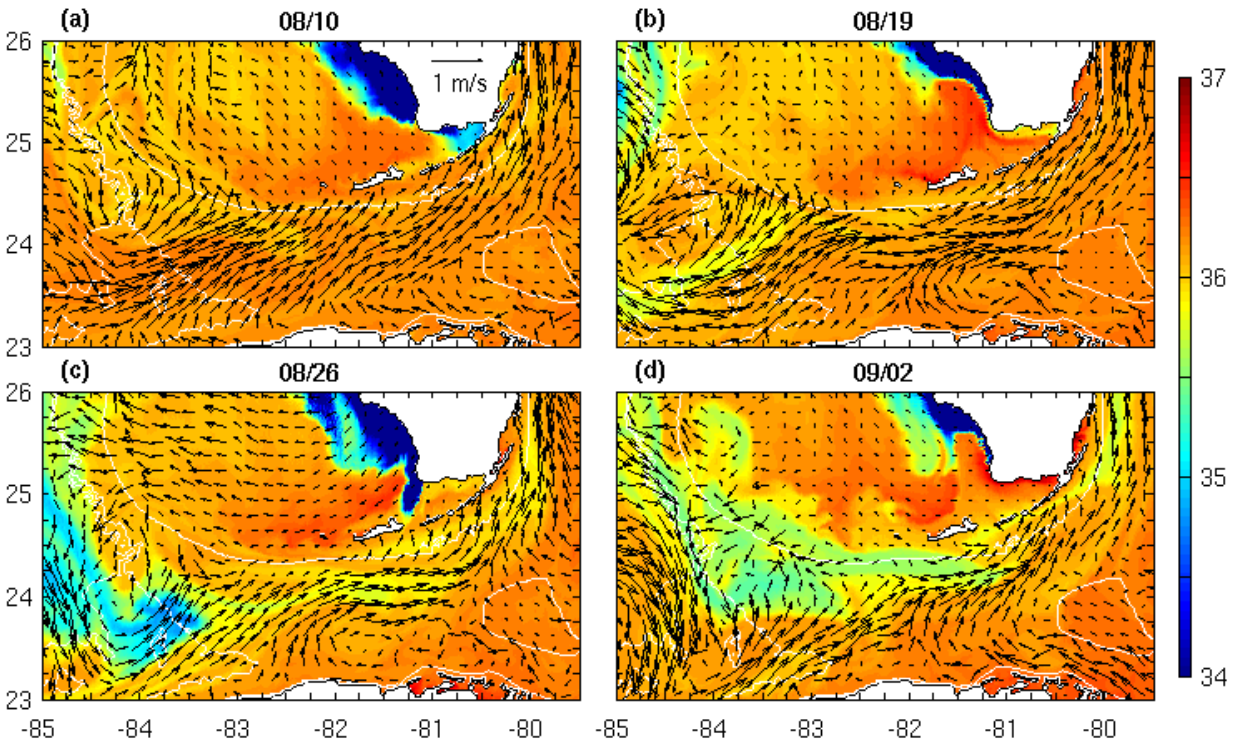

Figure 11: Snapshots of the 1/50° GoM reanalysis Sea Surface Salinity (surfaces) with surface currents (vectors), on (a) August 10, (b) August 19, (c) August 26, and (d) September 2, 2014. Zoom on the southern part of the WFS. Current vectors are plotted every eight model grid points. White lines indicate the 200, 2000, and 3000 m isobaths.

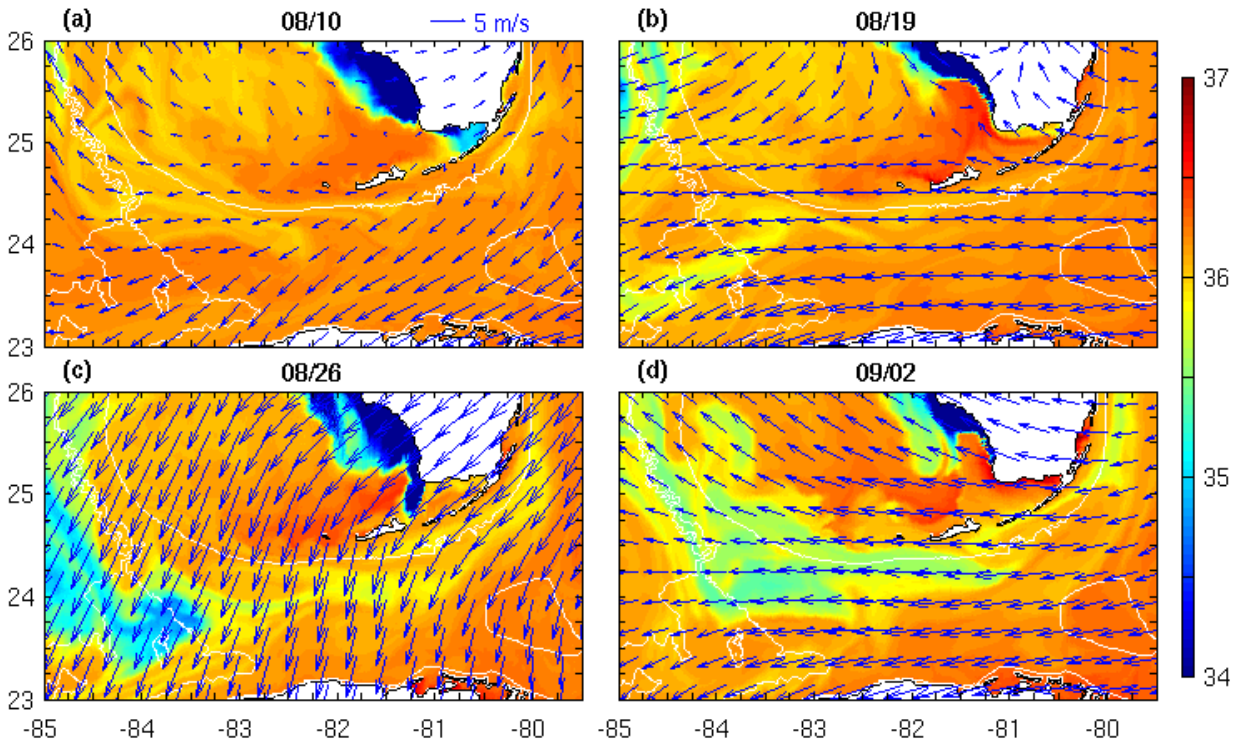

Figure 12: Snapshots of the 1/50° GoM reanalysis Sea Surface Salinity (surfaces) with 10 m wind from the NAVy Global Environmental Model (NAVGEM), on the same dates as Figure 11: (a) August 10, (b) August 19, (c) August 26, and (d) September 2, 2014 Wind vectors are plotted every 15 model grid points. White lines indicate the 200, 2000, and 3000 m isobaths.

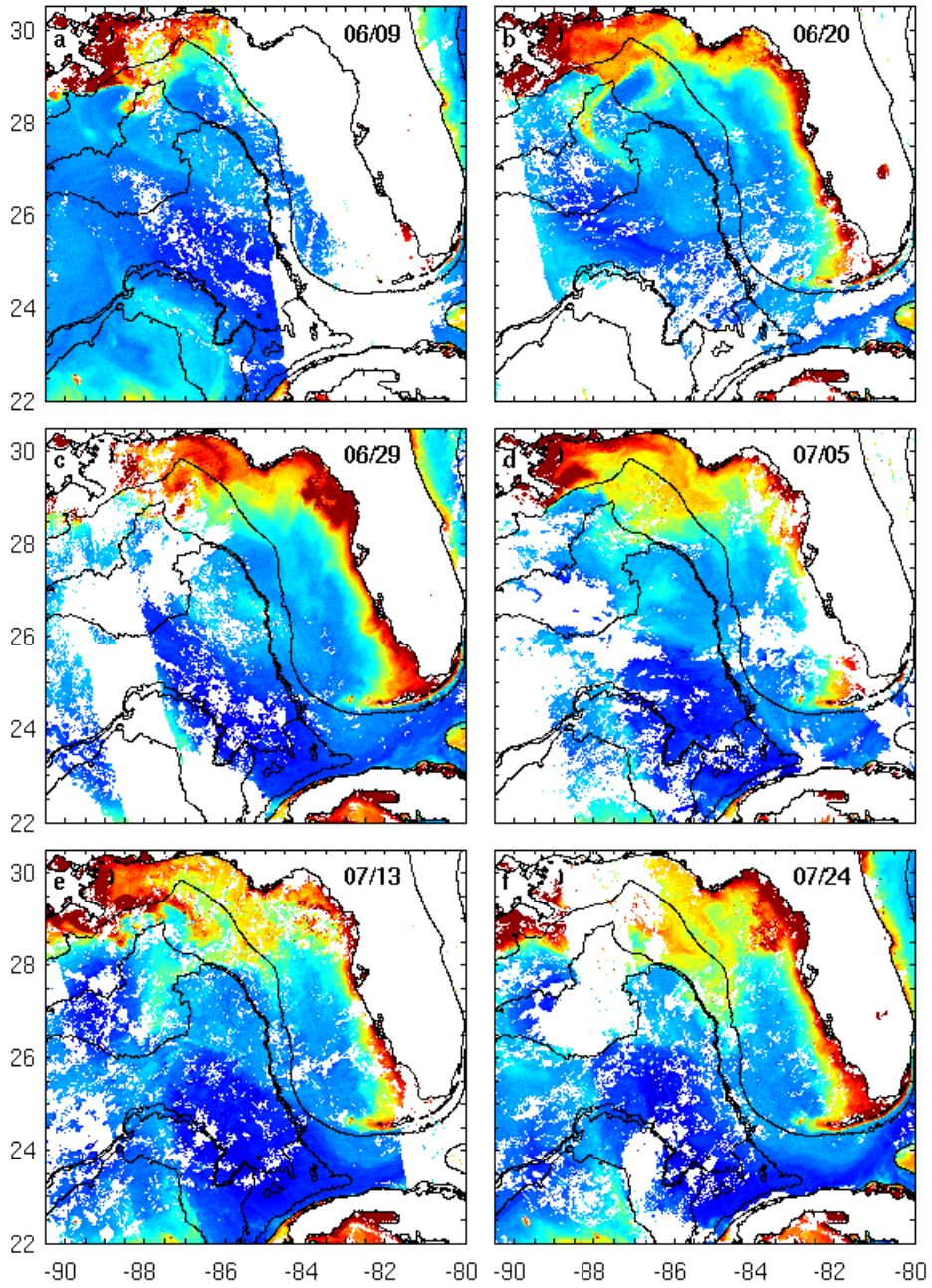

Figure 13: Three-day composite maps of chlorophyll-a (chl-a) derived from the NASA Modis Aqua satellite data on the same days as Figure 9: (a) June 9, (b) June 20, (c) June 29, (d) July 5, (e) July 13, and (f) July 24. Black lines represent the 200, 2000, and 3000 m isobaths.

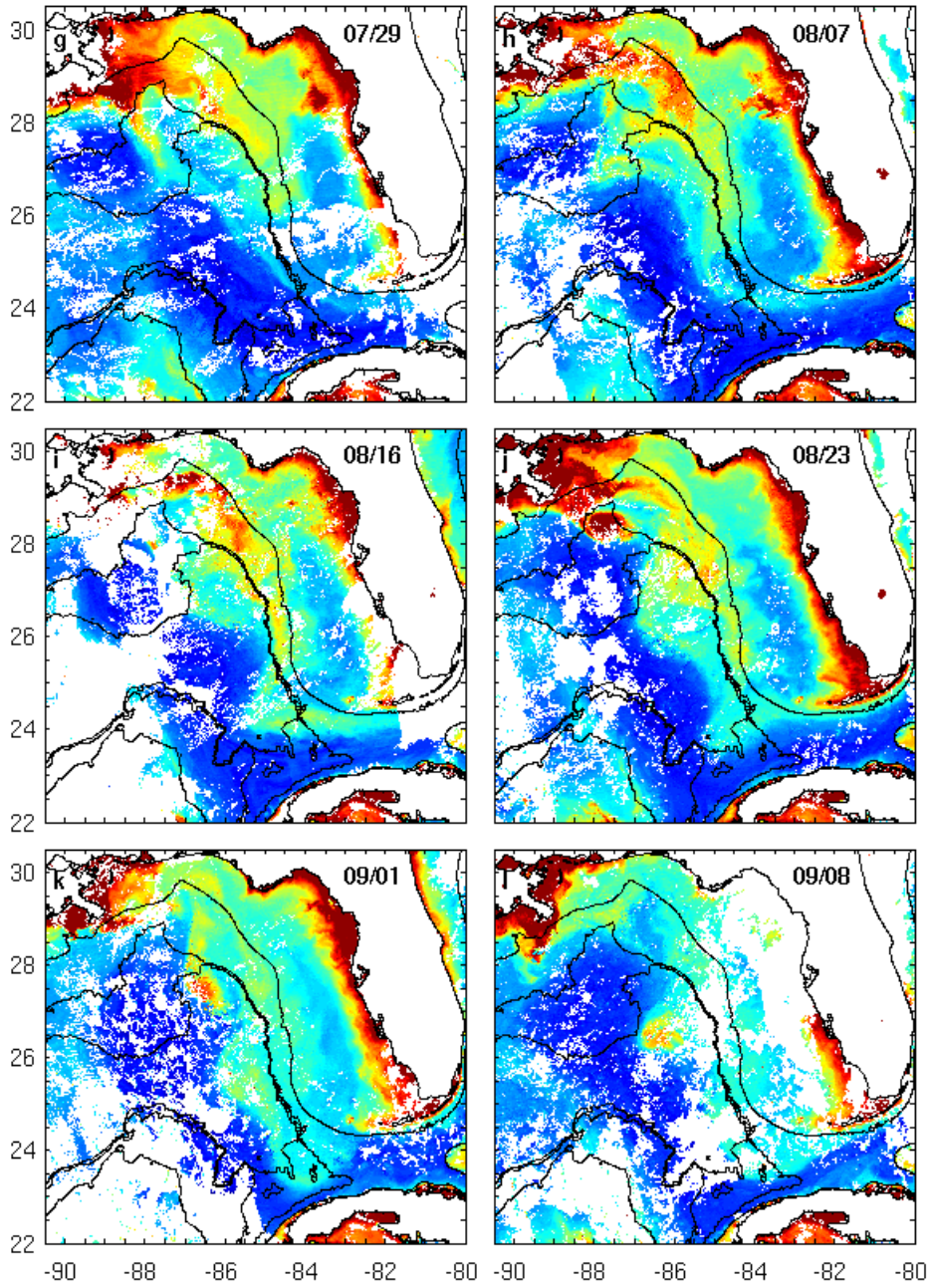

Figure 13 (continued): Three-day composite maps of chlorophyll-a (chl-a) derived from the NASA Modis Aqua satellite data on the same days as Figure 9: (g) July 29, (h) August 7, (i) August 16, (j) August 23, (k) September 1, and (l) September 8. Black lines represent the 200, 2000, and 3000 m isobaths.

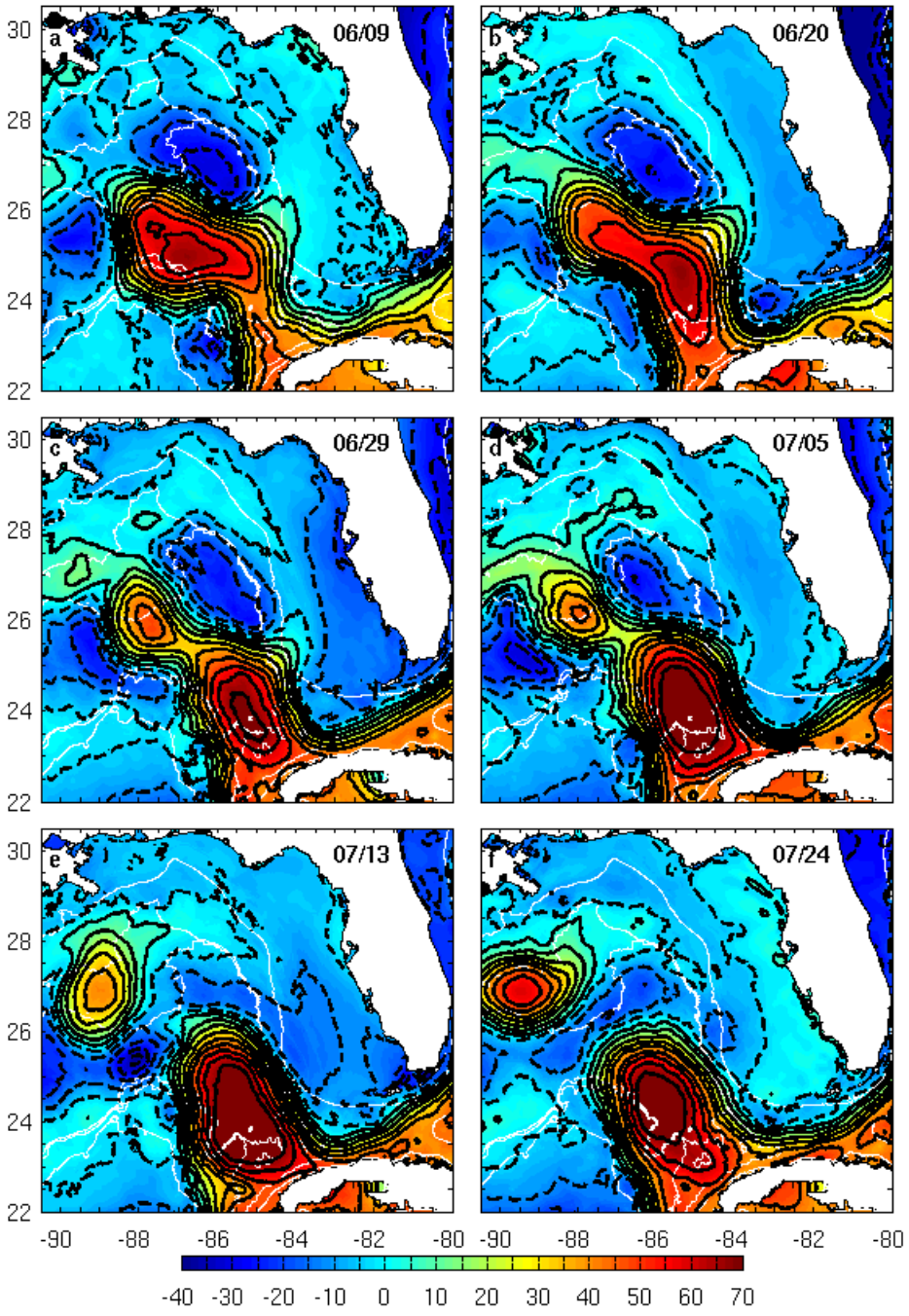

Figure 14: Snapshots of the 1/50° GoM-HYCOM reanalysis Sea Surface Height (zoom on the eastern GoM) corrected from the instantaneous mean over the Gulf of Mexico on the same dates as Figure 9: (a) June 9, (b) June 20, (c) June 29, (d) July 5, (e) July 13, and (f) July 24. The thick black lines are the SSH contours, with continuous lines for positive SSH, and dashed lines for negative SSH. White lines represent the 200, 2000, and 3000 m isobaths.

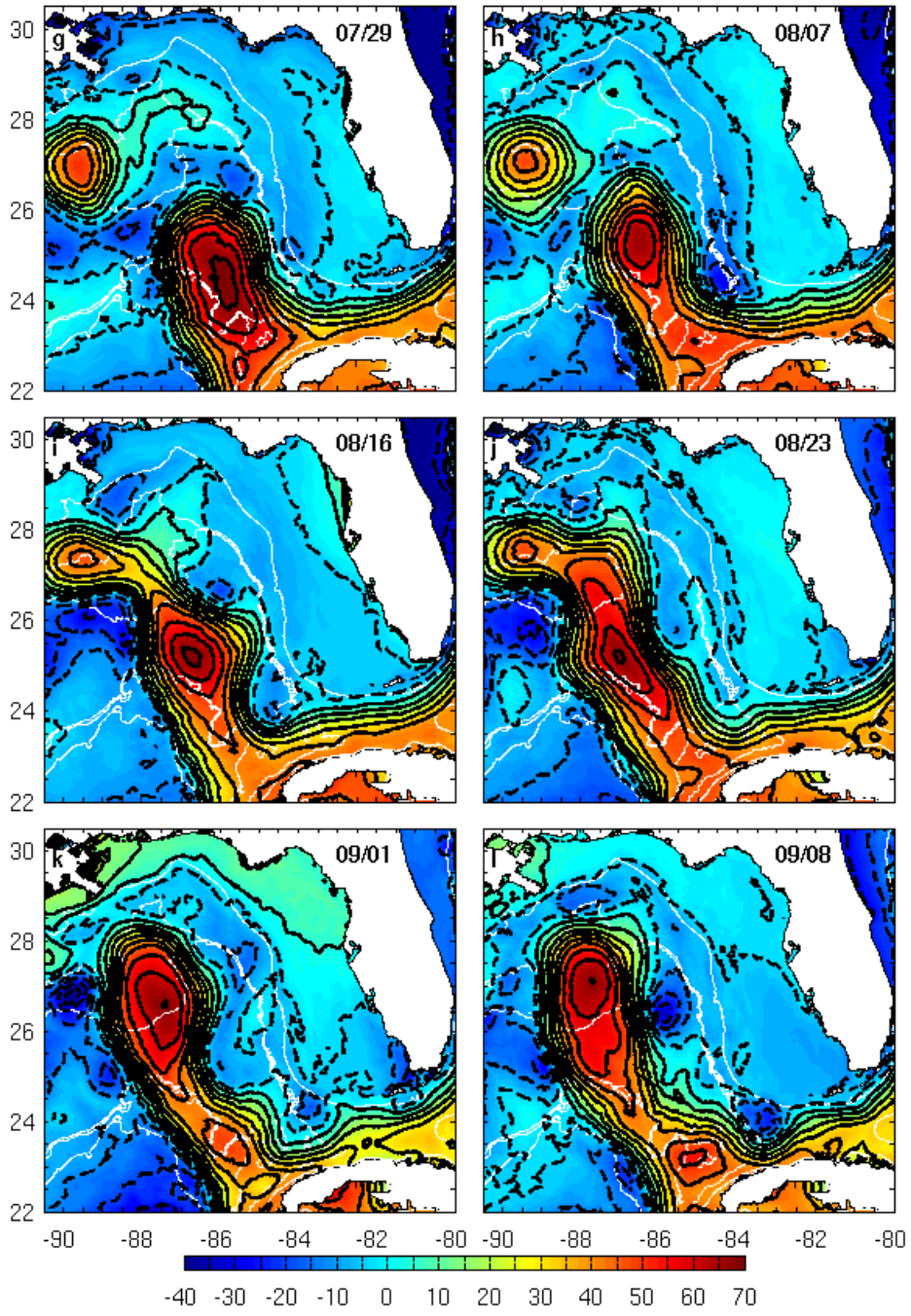

Figure 14 (continued): Snapshots of the 1/50° GoM-HYCOM reanalysis Sea Surface Height (zoom on the eastern GoM) corrected from the instantaneous mean over the Gulf of Mexico on the same dates as Figure 9: (g) July 29, (h) August 7, (i) August 16, (j) August 23, (k) September 1, and (l) September 8. The thick black lines are the SSH contours, with continuous lines for positive SSH, and dashed lines for negative SSH. White lines represent the 200, 2000, and 3000 m isobaths.

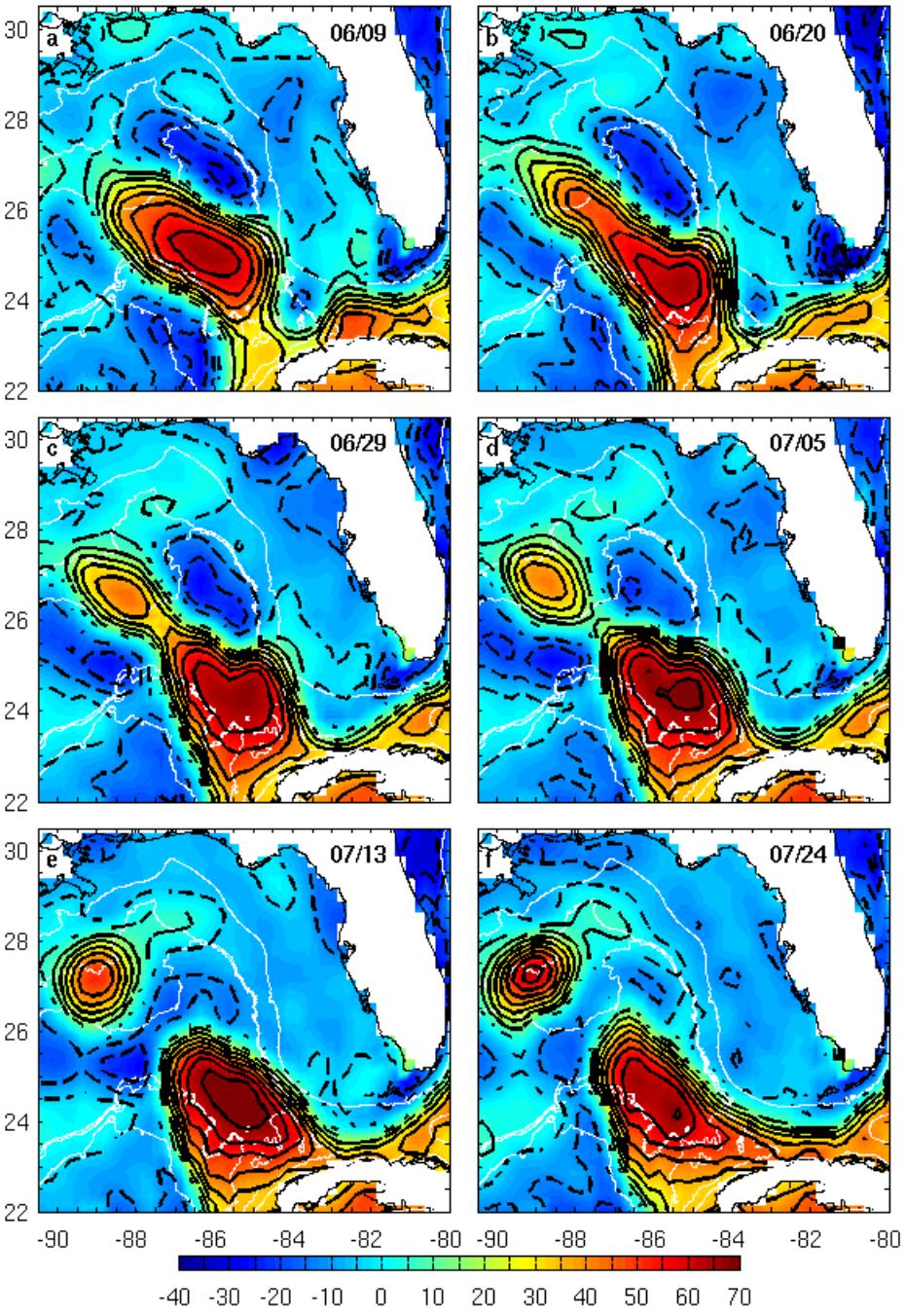

Figure 15: Observed Mapped Absolute Dynamic Topography (MADT) corrected from the instantaneous mean over the Gulf of Mexico on the same dates as Figure 9: (a) June 9, (b) June 20, (c) June 29, (d) July 5, (e) July 13, and (f) July 24. The thick black lines are the MADT contours, with continuous lines for positive MADT, and dashed lines for negative MADT. White lines represent the 200, 2000, and 3000 m isobaths.

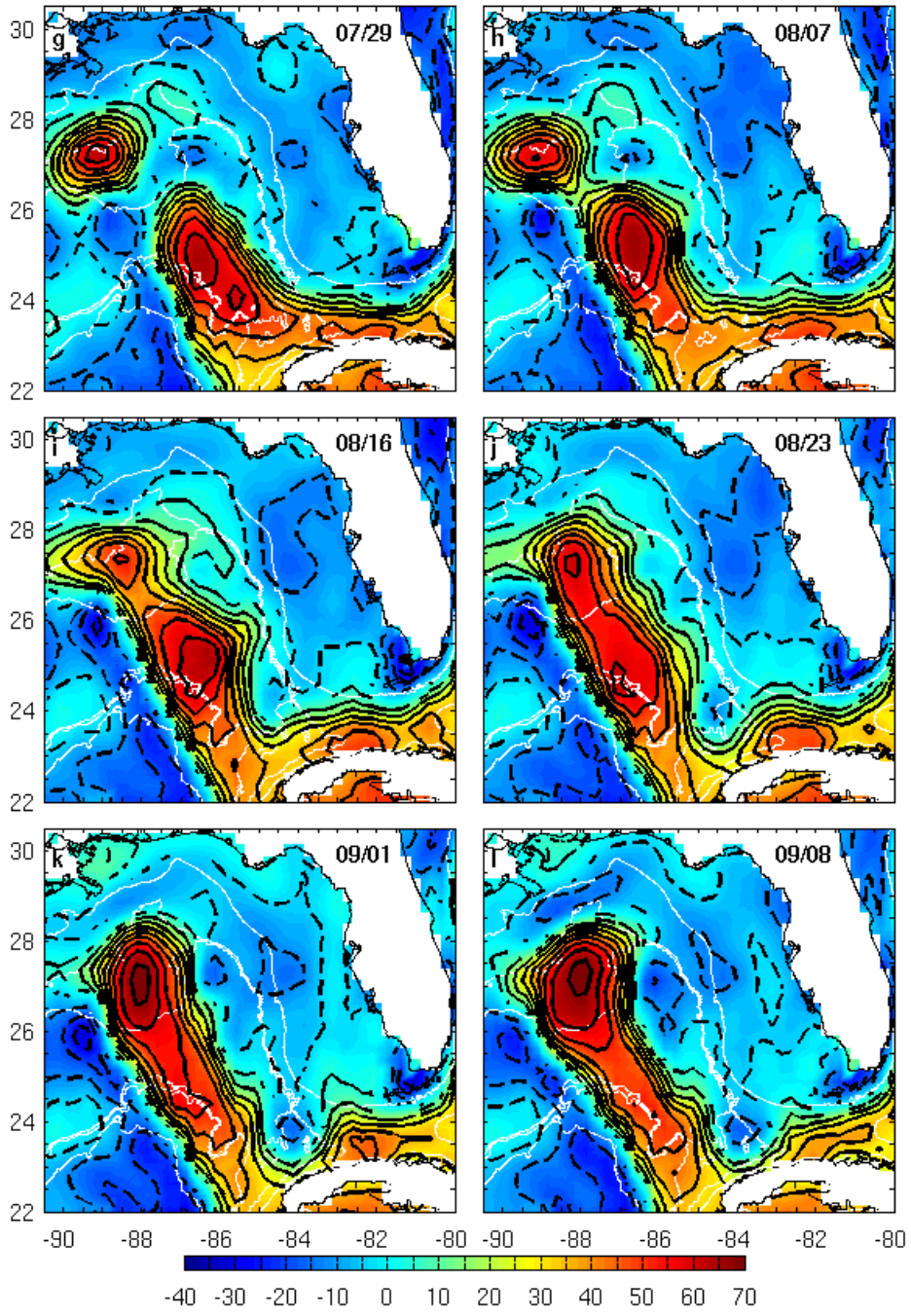

Figure 15 (continued): Observed Mapped Absolute Dynamic Topography (MADT) corrected from the instantaneous mean over the Gulf of Mexico on the same dates as Figure 9: (g) July 29, (h) August 7, (i) August 16, (j) August 23, (k) September 1, and (l) September 8. The thick black lines are the MADT contours, with continuous lines for positive MADT, and dashed lines for negative MADT. White lines represent the 200, 2000, and 3000 m isobaths.

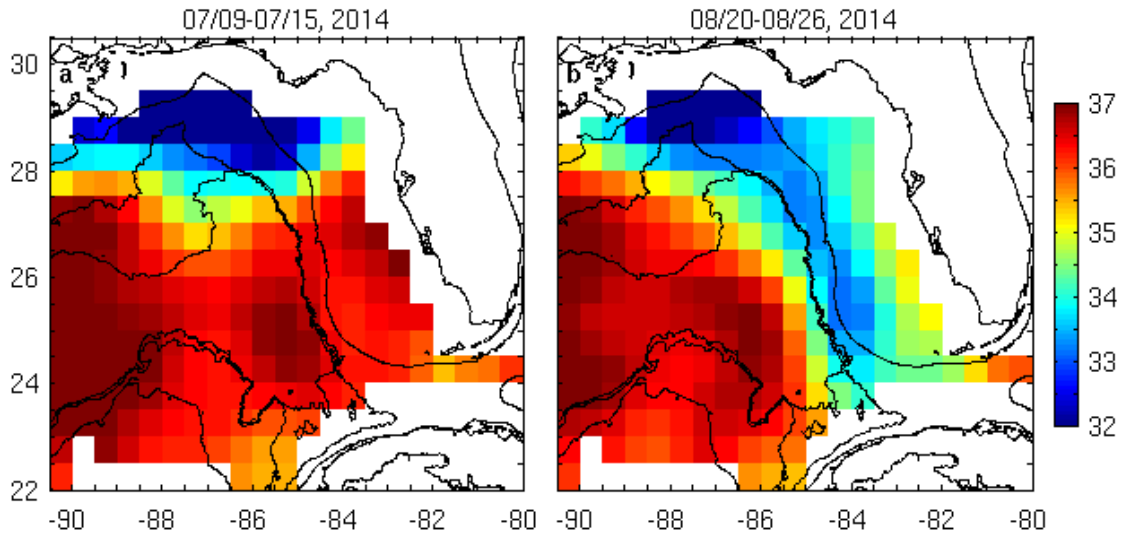

Figure 16: Weekly map of Sea Surface Salinity observed by SMOS for the weeks: (a) July 9-15, and (b) August 20-26, 2014. Black lines represent the 200, 2000, and 3000 m isobaths.